

WL-TR-97-4110

LOW FRICTION AND WEAR SURFACE FOR APPLICATION  
OVER A WIDE RANGE OF TEMPERATURE



Rabi S. Bhattacharya, Ph.D.

UES, Inc.  
4401 Dayton-Xenia Road  
Dayton, OH 45432-1894

June 1997

Final Report for: 9/27/96 - 5/26/97

**This is a Small Business Innovation Research (SBIR) Phase I Report**

Approved for Public Release; Distribution is Unlimited

THIS QUALITY INSPECTED &

MATERIALS DIRECTORATE  
WRIGHT LABORATORY  
AIR FORCE MATERIEL COMMAND  
WRIGHT-PATTERSON AIR FORCE BASE, OH 45433-7734

19980108 074

## NOTICE

USING GOVERNMENT DRAWINGS, SPECIFICATIONS, OR OTHER DATA INCLUDED IN THIS DOCUMENT FOR ANY PURPOSE OTHER THAN GOVERNMENT PROCUREMENT DOES NOT IN ANY WAY OBLIGATE THE US GOVERNMENT. THE FACT THAT THE GOVERNMENT FORMULATED OR SUPPLIED THE DRAWINGS, SPECIFICATIONS, OR OTHER DATA DOES NOT LICENSE THE HOLDER OR ANY OTHER PERSON OR CORPORATION; OR CONVEY ANY RIGHTS OR PERMISSION TO MANUFACTURE, USE, OR SELL ANY PATENTED INVENTION THAT MAY RELATE TO THEM.

THIS REPORT IS RELEASABLE TO THE NATIONAL TECHNICAL INFORMATION SERVICE (NTIS). AT NTIS, IT WILL BE AVAILABLE TO THE GENERAL PUBLIC, INCLUDING FOREIGN NATIONS.

THIS TECHNICAL REPORT HAS BEEN REVIEWED AND IS APPROVED FOR PUBLICATION.



MING Y. CHEN, Project Engineer  
Nonstructural Materials Branch  
Nonmetallic Materials Division



WAYNE E. WARD, Acting Chief  
Nonstructural Materials Branch  
Nonmetallic Materials Division



ROBERT L. RAPSON, Chief  
Nonmetallic Materials Division  
Materials Directorate

IF YOUR ADDRESS HAS CHANGED, IF YOU WISH TO BE REMOVED FROM OUR MAILING LIST, OR IF THE ADDRESSEE IS NO LONGER EMPLOYED BY YOUR ORGANIZATION PLEASE NOTIFY WL/MLBT WRIGHT-PATTERSON AFB OH 45433-7734 TO HELP MAINTAIN A CURRENT MAILING LIST.

Do not return copies of this report unless contractual obligations or notice on a specific document requires its return.

# REPORT DOCUMENTATION PAGE

Form Approved  
OMB No. 0704-0188

Public reporting burden for this collection of information is estimated to average 1 hour per response, including the time for reviewing instructions, searching existing data sources, gathering and maintaining the data needed, and completing and reviewing the collection of information. Send comments regarding this burden estimate or any other aspect of this collection of information, including suggestions for reducing this burden, to Washington Headquarters Services, Directorate for Information Operations and Reports, 1215 Jefferson Davis Highway, Suite 1204, Arlington, VA 22202-4302, and to the Office of Management and Budget, Paperwork Reduction Project (0704-0188), Washington, DC 20503.

1. AGENCY USE ONLY (Leave blank)		2. REPORT DATE June 1997		3. REPORT TYPE AND DATES COVERED Final Report, 09/27/96 - 05/26/97	
4. TITLE AND SUBTITLE Low Friction and Wear Surface for Application Over a Wide Range of Temperature				5. FUNDING NUMBERS C: F33615-96-C-5086 PE: 65502F PR: 3005 TA: 5x WU: 08	
6. AUTHOR(S) Rabi S. Bhattacharya					
7. PERFORMING ORGANIZATION NAME(S) AND ADDRESS(ES) UES, Inc. 4401 Dayton-Xenia Road Dayton, OH 45432-1894				8. PERFORMING ORGANIZATION REPORT NUMBER	
9. SPONSORING/MONITORING AGENCY NAME(S) AND ADDRESS(ES) MATERIALS DIRECTORATE WRIGHT LABORATORY AIR FORCE MATERIEL COMMAND WRIGHT PATTERSON AFB OH 45433-7734 POC: MING Y. CHEN, WL/MLBT (937) 255-9099				10. SPONSORING/MONITORING AGENCY REPORT NUMBER WL-TR-97-4110	
11. SUPPLEMENTARY NOTES					
12a. DISTRIBUTION/AVAILABILITY STATEMENT Approved for public release; distribution is unlimited				12b. DISTRIBUTION CODE	
13. ABSTRACT (Maximum 200 words) REPORT DEVELOPED UNDER SBIR CONTRACT There is a strong demand for solid lubricant coatings that can function over a wide range of temperatures. Since no one material can provide adequate lubricating properties over a wide temperature range, an approach of a composite coating was evaluated in Phase I. Composite coatings of ZnO and MoS <sub>2</sub> were deposited by sputtering on M50 steel and Si <sub>3</sub> N <sub>4</sub> substrates. Coatings were characterized by Rutherford back scattering (RBS), Auger electron spectroscopy (AES) and Transmission electron microscopy (TEM), both before and after exposure to high temperatures (up to 700°C) in air. Friction measurements were performed at temperatures in the range of room temperature to 700°C in air. Results indicate that layered ZnO+MoS <sub>2</sub> /ZnO coating performed better at high temperature than the mixed composite coatings. Friction coefficients were in the range 0.2 to 0.3 at temperatures below 400°C for coated M50 substrate against uncoated M50 ball. At higher temperatures, the friction coefficient increased to ≥0.4 for coated Si <sub>3</sub> N <sub>4</sub> substrate against uncoated Si <sub>3</sub> N <sub>4</sub> ball.					
14. SUBJECT TERMS SBIR REPORT Solid lubricant, Coatings, Friction, Wear, ZnO, MoS <sub>2</sub> , Lubrication				15. NUMBER OF PAGES 45	
				16. PRICE CODE	
17. SECURITY CLASSIFICATION OF REPORT Unclassified	18. SECURITY CLASSIFICATION OF THIS PAGE Unclassified	19. SECURITY CLASSIFICATION OF ABSTRACT Unclassified	20. LIMITATION OF ABSTRACT SAR		

## **PREFACE**

This research was funded by the U.S. Air Force under a Phase I SBIR program, Contract No. F33615-96-C-5086. The work described herein was carried out by UES, Inc. during the project period from 09/27/96 - 05/26/97, including a two-month extension. The Air Force project engineer was Dr. Ming Y. Chen.

## ACKNOWLEDGMENT

The author of this report wishes to acknowledge the contributions of Dr. A.K. Rai of UES in characterization, and Dr. P. Blau and Mr. C. Yust of Oak Ridge National Laboratory for high temperature friction measurements. The work reported here has been supported by the following Small Business Innovative Research (SBIR) Program: Department of Defense - Contract No. F33615-96-C-5086, Contract Monitor - Ming Chen.

## TABLE OF CONTENTS

<u>SECTION</u>	<u>PAGE</u>
PREFACE .....	ii
ACKNOWLEDGMENT .....	iii
LIST OF ILLUSTRATIONS .....	v
LIST OF TABLES .....	vi
1.0 INTRODUCTION .....	1
2.0 RESEARCH OBJECTIVES .....	2
3.0 RESEARCH WORK CARRIED OUT .....	3
3.1 Experimental Description .....	3
3.1.1 Selection of Solid Lubricants .....	3
3.1.2 Deposition of Coatings by Sputtering .....	3
3.1.3 Coating Characterizations .....	5
3.1.4 Friction and Wear Tests .....	6
4.0 RESULTS .....	7
4.1 Film Depositions and Characterizations .....	7
4.2 Friction Test Results .....	23
4.3 Discussion of Results .....	33
5.0 POTENTIAL APPLICATIONS .....	38
REFERENCES .....	38

## LIST OF ILLUSTRATIONS

<b>FIGURE</b>		<b>PAGE</b>
1	Schematic Diagram of the High Temperature Tribometer .....	6
2	RBS Spectrum of ZnO Film .....	10
3	RBS Spectrum of Composite Film #1 .....	12
4	RBS Spectrum of Composite Film #2 .....	13
5	RBS Spectrum of Composite Film #3 .....	14
6	RBS Spectrum of Composite Film #4 .....	15
7	RBS Spectrum of Composite Film #5 .....	16
8	Auger Sputter Profiles of Sample #3, (a) As-deposited, (b) After Annealing at 600°C for 2 Hours .....	19
9	Auger Sputter Profiles of Sample #5, (a) As-deposited, (b) After Annealing at 600°C for 2 Hours .....	20
10	Cross-section Transmission Electron Micrographs of Composite Film #5, (a) Bright-field, (b) Dark-Field .....	21
11	The Selected Area Diffraction Pattern of Composite Film #5 .....	21
12	Auger Sputter Profiles of Sample #6, As-deposited .....	24
13a	Auger Sputter Profiles of Sample #6, After Annealing, 500°C, 1 Hour .....	25
13b	Auger Sputter Profiles of Sample #6, After Annealing, 600°C, 1 Hour .....	26
13c	Auger Sputter Profiles of Sample #6, After Annealing, 600°C, 3 Hours .....	27
14	Friction Coefficient as a Function of Time for Sample #1 .....	28
15	Friction Coefficient as a Function of Time for Sample #2 .....	29
16	Friction Coefficient as a Function of Time for Sample #3 .....	30
17	Friction Coefficient as a Function of Time for Sample #4 .....	31
18	Friction Coefficient as a Function of Time for Sample #5 .....	32
19	Friction Coefficient as a Function of Time for Sample #6 .....	34
20	Friction Coefficient as a Function of Time for ZnO Film on M50 .....	35
21	Friction Coefficient as a Function of Time for MoS <sub>2</sub> Film on M50 .....	36
22	Optical Micrograph of the Sample #5 After Friction Tests at 400°C .....	37

## LIST OF TABLES

<u>TABLE</u>		<u>PAGE</u>
1	Friction Coefficients of Oxides .....	4
2	Parameters for Theoretical Fit of the RBS Spectrum of Figure 2 .....	9
3	Parameters for Theoretical Fit of the RBS Spectrum of Figure 3 .....	17
4	Parameters for Theoretical Fit of the RBS Spectrum of Figure 4 .....	17
5	Parameters for Theoretical Fit of the RBS Spectrum of Figure 5 .....	17
6	Parameters for Theoretical Fit of the RBS Spectrum of Figure 6 .....	17
7	Parameters for Theoretical Fit of the RBS Spectrum of Figure 7 .....	18
8	Observed d-values Compared to the Known d-values from X-ray Diffraction of Powders .....	22
9	Layer Thicknesses .....	22

## 1.0 INTRODUCTION

Advanced jet engines require lubricants that can function over a wide range of temperatures, subambient to 800°C. Lubrication at such wide temperature range can only be attained by using appropriate solid lubricants. The maximum useful temperature for most common solid lubricants such as MoS<sub>2</sub>, WS<sub>2</sub>, etc., is limited to about 400°C under favorable conditions in air [1]. In vacuum applications, however, these materials can be used at higher temperatures (~600°C).

Another common lubricant is graphite which requires the presence of water or hydrocarbons to develop good lubricating properties. Graphite lubricates at room temperature and above 425°C but not at intermediate temperatures. Low friction at room temperature is attributed to the beneficial effect of absorbed moisture. High friction at intermediate temperature is attributed to desorption of water and possibly other gases. Low friction above 425°C is attributed to interaction of graphite with oxides of the lubricated metal. Graphite itself begins to oxidize at about 400°C.

Over the years, some unconventional solid lubricants based on oxides and fluorides have been identified for high temperature applications [2,3]. These are: MoO<sub>3</sub>, TiO<sub>x</sub>, CoO, ZnO, ZrO<sub>2</sub>, LiF, CaF<sub>2</sub>, BaF<sub>2</sub>. Use of oxides and fluorides has been limited because of their lubricating ability within a narrow temperature range. Also, the friction coefficient of most of these oxides even at high temperatures is rather high, ~0.2-0.4.

A new class of materials belonging to complex metal chalcogenides have recently been identified for high temperature applications [4]. Two compositions, in particular, have shown superior thermal, oxidative and tribological properties over a broad temperature range up to 650°C. These are: cesium oxytrithiotungstate and zinc oxytrithiomolybdate. The friction coefficients reported so far using these lubricants are in the range 0.15 - 0.37 depending on the temperature. Usually higher friction coefficient was found at lower temperature. These lubricants apparently degrade at temperatures greater than 650°C.

There is a great need, therefore, to develop a solid lubricant coating that can operate at temperatures from ambient (room temperature) to high temperature, 800°C. The objective of this study was to explore the concept of encapsulation of low temperature lubricants such as MoS<sub>2</sub> and WS<sub>2</sub> with high temperature oxide lubricants. It is expected that the oxide lubricant phase will protect MoS<sub>2</sub> or WS<sub>2</sub> from oxidation at high temperature while providing a low friction corresponding to that of MoS<sub>2</sub> or WS<sub>2</sub> by dynamic exposure of these materials in the contact region. Also, it is possible that a metal-molybdate or tungstate can form in the contact region during friction at high temperatures. Some of these molybdates and tungstates are quite stable at high temperature under oxidizing environment, and can provide low friction. For example, Zabinski et al [5] have studied the composite films of PbO-MoS<sub>2</sub> by pulsed laser deposition. Crystalline PbMoO<sub>4</sub>, MoS<sub>2</sub>, and MoO<sub>3</sub> were produced after the films were annealed in air at 500°C. PbMoO<sub>4</sub> has been known to possess lubricating properties at elevated temperatures.

The work performed at UES, Inc. under this SBIR Phase I program funded by BMDO consisted of depositing composite coatings of MoS<sub>2</sub> and ZnO by sputtering, characterization of these coatings for composition and microstructure and evaluation of their friction coefficients in the temperature range, room temperature to 800°C.

## **2.0 RESEARCH OBJECTIVES**

The Phase I research objectives consisted of establishing conditions for depositing composite films of MoS<sub>2</sub> and an oxide lubricant. For Phase I feasibility studies we proposed to use ZnO as an oxide lubricant. Sputtering techniques was proposed for the fabrication of the coatings. Rutherford backscattering spectroscopy (RBS), and Transmission electron microscopy (TEM) were proposed for the analysis of composition and microstructure, respectively. Friction and wear characteristics of these coatings at room and elevated temperatures were proposed to be evaluated by using pin-on-disc machine. The specific objectives of Phase I, as enumerated in the proposal, are as follows:

1. Prepare sputter targets of compositions  $\text{MoS}_2$ :Oxide as 1:1, 0.25:1 and 0.1:1.
2. Deposit coatings by sputter deposition.
3. Characterize the films for composition and microstructure by using RBS and TEM techniques, respectively.
4. Perform friction and wear tests at temperatures in the range room to  $800^\circ\text{C}$ .

### **3.0 RESEARCH WORK CARRIED OUT**

#### **3.1 EXPERIMENTAL DESCRIPTION**

##### **3.1.1 Selection of Solid Lubricants**

$\text{MoS}_2$  is a well known low temperature ( $<350^\circ\text{C}$ ) solid lubricant.  $\text{ZnO}$  is chosen as the higher temperature oxide lubricant. It is well known that ductile oxide films provide good wear protection at high temperature and at the same time prevent excessive oxidation [6]. Usually, the oxides with low hardness at room temperature are highly ductile at high temperature. Under pressure, the ductile oxide will smear over the surface and prevent direct contact of the bare sliding surfaces. Some oxides with low hardness at room temperature are:  $\text{Re}_2\text{O}_7$ ,  $\text{MoO}_3$ ,  $\text{BaO}$ ,  $\text{V}_2\text{O}_5$ ,  $\text{CaO}$ ,  $\text{ZnO}$  and  $\text{CuO}$ . Friction coefficient of these and other similar oxides against various counterface materials have been assembled in Table 1. From these, we chose  $\text{ZnO}$  to verify the concept presented in this proposal. The selection is primarily based on its low friction coefficient at high temperature and high melting temperature.

##### **3.1.2 Deposition of Coatings by Sputtering**

Coatings were deposited by sputtering since sputtering is known to provide high quality, highly reproducible coatings. Sputtering is a process whereby material is dislodged and ejected

Table 1. Friction Coefficients of Oxides

Oxide	Temp °C	Friction Coefficient	Ref.
Re <sub>2</sub> O <sub>7</sub>	316	.23	33
MoO <sub>3</sub>	700	.20	33
	595	.27	34
WO <sub>3</sub>	800	.39	34
	700	.55	35
	600	.56	33
V <sub>2</sub> O <sub>5</sub>	600	.32	33
ZnO	700	.33	35
CuO	600	.22	33
	600	.25	36
B <sub>2</sub> O <sub>3</sub>	650	.14	35
			37
CeO <sub>2</sub>	>800	.20	38
CaO	700	.20	39
CuMoO <sub>4</sub>	600	.28	36
CoMoO <sub>4</sub>	600	.37	36
	800	.27	34
NiMoO <sub>4</sub>	700	.29	35
CuWO <sub>4</sub>	700	.41	35
FeWO <sub>4</sub>	700	.43	35
NiWO <sub>4</sub>	700	.51	35
CoWO <sub>4</sub>	800	.20	34

from the surface of a solid due to the momentum exchange associated with surface bombardment by energetic particles. Sputter deposition is a vacuum coating process [7]. The coating material called the target is placed into a vacuum chamber along with the substrates and the chamber is evacuated to a pressure typically in the range of  $10^{-6}$  to  $10^{-8}$  torr. The bombarding species are generally ions of a heavy inert gas such as argon. The sputtered material is ejected primarily in atomic form. The substrates are positioned in front of the target so that they are coated with the flux of sputtered atoms. An evacuated chamber is filled with the inert gas to a pressure of 1 to 100 mtorr and electric discharge is ignited so that an ionization of the working gas is produced in the region adjacent to the target.

In this program, we have used an ultra-high vacuum system equipped with two 3-inch magnetron guns. Composite coatings of MoS<sub>2</sub> and ZnO were prepared by simultaneous sputtering of MoS<sub>2</sub> using DC and ZnO using RF power. The powers were independently controlled to vary the rates of sputtering to obtain coatings of different compositions and microstructures.

### **3.1.3 Coating Characterizations**

A variety of characterization techniques were used to analyze the composition, microstructure, and morphology of the deposited coatings.

#### **Rutherford Backscattering (RBS)**

RBS analysis was used to obtain information on the composition as a function of depth of the coatings. RBS spectra were acquired at the 160° detector with the sample surface perpendicular to the incident ion beam. The spectra obtained at the 160° detector in the RBS arrangement allow a precise determination of layer thicknesses and composition.

#### **Auger Electron Spectroscopy (AES)**

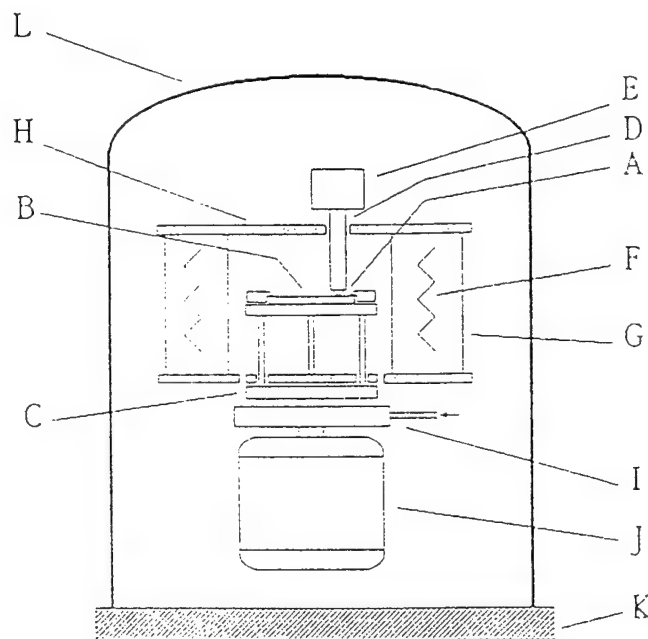
AES was used in combination with sputtering to analyze the composition as a function of depth of the coatings. For low mass atoms such as oxygen, AES is more sensitive than RBS.

#### **Microstructural Characterization**

The as-deposited coatings were characterized by scanning transmission electron microscopy (STEM), in conjunction with energy dispersive x-ray analysis (EDAX), to identify the morphology, structure and composition of the surface.

### 3.1.4 Friction and Wear Tests

The friction tests were performed in a high-temperature test system at the Oak Ridge National Laboratory. The system utilized the pin-on-disc wear test geometry and is fitted with a resistance heater furnace capable of providing test temperatures up to 1000°C, shown in Figure 1. Either M50 or Si<sub>3</sub>N<sub>4</sub> spheres of about 9.5 mm diameter were held in the end of a rod fixed to a yoke supported by strain gauged force transducers. The test discs were clamped against a rotation system driven by a variable speed motor. The force transducers provide continuous measurement of both normal and tangential forces. Load was applied to the pin by dead-weight loading. The friction and wear of the coated specimens were evaluated at room temperature, 400°C and 600°C. The tests were performed in air with humidity in the range 45-55%. A fixed load of 1 N and an average sliding velocity of 0.1 m/sec were used for these tests.



—Schematic diagram of the controlled-atmosphere high-temperature test system. (A) sphere used as pin member held in rod (D); (B) disc clamped to top of rotating stage (C); (E) terminus of pin rod and location of normal and tangential force transducers; (F) heating elements enclosed within quartz cylinders, the outer cylinder (G) coated with gold; (H) insulation at top and bottom of furnace; (I) water-cooled plate; (J) variable speed drive motor; (K) baseplate for system on which enclosure (L) is seated.

Figure 1. Schematic Diagram of the High Temperature Tribometer.

## 4.0 RESULTS

### 4.1 FILM DEPOSITIONS AND CHARACTERIZATIONS

A number of depositions were performed after some initial trials to set-up the rf power supply with proper grounding of the chamber. Initially, a film of ZnO was deposited by using rf sputtering under the following conditions:

Film = ZnO

Chamber Base Pressure =  $5 \times 10^{-7}$  torr

Forward Power = 400 W

Reflected Power = 50 W

DC Bias = -130 V

Argon Flow Rate = 50 SCCM

Argon Pressure = 7.5 mtorr

The films were deposited on smooth silicon and M50 steel substrates. The deposition rate at a distance of about 20 cm from the target was found to be 20 Å/min. The distance correspond to the focal point of both guns.

Subsequent depositions were performed using both guns to deposit a composite MoS<sub>2</sub> and ZnO films. Following conditions were used in depositing the films:

#### Composite Film #1

##### **ZnO**

Chamber Base Pressure =  $6 \times 10^{-7}$  torr

Forward Power = 400 W

Reflected Power = 5 W

DC Bias = -160 V

Argon Flow Rate = 50 SCCM

Argon Pressure = 8.5 mtorr

Deposition Time = 120 min.

##### **MoS<sub>2</sub>**

Power = 50 W

Composite Film #2

**ZnO**

Chamber Pressure =  $6.5 \times 10^{-7}$  torr

Forward Power = 400 W

Reflected Power = 40 W

DC Bias = -145 V

Argon Flow Rate = 50 SCCM

Argon Pressure = 7.7 mtorr

Deposition Time = 100 min.

**MoS<sub>2</sub>**

Power = 20 W

Composite Film #3

**ZnO**

Chamber Pressure =  $7.5 \times 10^{-7}$  torr

Forward Power = 400 W

Reflected Power = 60 W

DC Bias = -140 V

Argon Flow Rate = 50 SCCM

Argon Pressure = 8.6 mtorr

Deposition Time = 100 min.

**MoS<sub>2</sub>**

Power = 10 W

Composite Film #4

**ZnO**

Chamber Base Pressure =  $7 \times 10^{-7}$  torr

Forward Power = 400 W

Reflected Power = 10 W

DC Bias = -160 V

Argon Flow Rate = 50 SCCM

Argon Pressure = 8 mtorr

Deposition Time = 100 min.

**MoS<sub>2</sub>**

Power = 5 W

### Composite Film #5

#### **ZnO**

Chamber Base Pressure =  $6 \times 10^{-7}$  torr

Forward Power = 400 W

Reflected Power = 25 W

DC Bias = -180 V

Argon Flow Rate = 50 SCCM

Argon Pressure = 8 mtorr

Deposition Time = 100 min.

#### **MoS<sub>2</sub>**

Power = 2 W

As can be seen from the above, the conditions for rf sputtering of ZnO were maintained about the same for all depositions while varying the power level of MoS<sub>2</sub> depositions. This is to incorporate various amounts of MoS<sub>2</sub> into ZnO matrix. Although we have tried to control the conditions for ZnO sputtering, the reflected power and the DC bias varied from run to run because of spurious interactions of rf with vacuum chamber components.

The film thicknesses were measured by surface profilometry and were found to be in the range 5000 Å to 7500 Å.

The films were analyzed for composition by using Rutherford Backscattering (RBS) analysis.

Figure 2 shows the RBS spectrum along with the theoretical fit (dotted line) of the ZnO film. The theoretical fits were obtained by assuming the parameters as shown in Table 2. Thus the composition of ZnO film is close to that of the target which is stoichiometric ZnO.

Table 2. Parameters for Theoretical Fit of the RBS Spectrum of Figure 2

Depth (Angstroms)	Atomic Concentration				
	O	Si	Zn	O/Zn	Density*
<2750	52.5	—	47.5	1.11	6.85E22
>	—	100	—	—	5.00E22

\*In units of atoms/cc

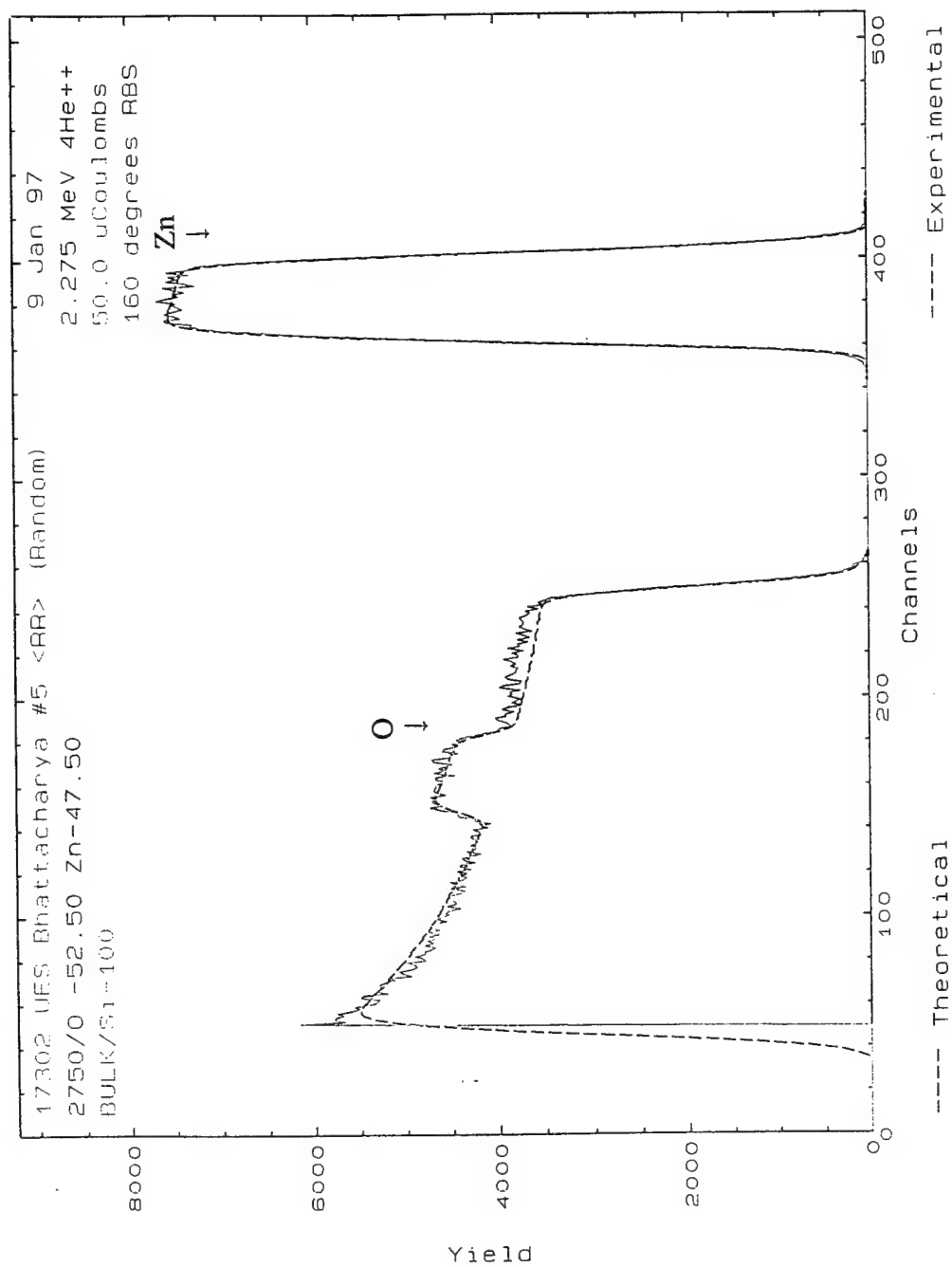


Figure 2. RBS Spectrum of ZnO Film.

Figures 3-7 show the RBS spectra corresponding to composite films #1 through #5. It should be noted that the composite film #5 was deposited by running the ZnO deposition continuously, but turning the MoS<sub>2</sub> deposition on for 10 minutes at every 10 minutes interval of a total of 100 min run. This has resulted in an oscillatory RBS spectrum indicating the layer structure of ZnO and ZnO+MoS<sub>2</sub> films. The results of the theoretical curve fitting of these spectra, Figures 3-7, are shown in Tables 3-7, respectively. The results indicate, in general, that there is excess oxygen present in these films. This is not unexpected since we have found earlier in our work that the sputtered MoS<sub>2</sub> film has the stoichiometry of MoS<sub>1.7</sub>O<sub>0.3</sub>.

Figures 8a and b show the Auger sputter profiles of sample #3 before and after exposure to 600°C for 2 hours. It is clearly evident that MoS<sub>2</sub> has totally oxidized losing all S. However, the analysis of sample #5, Figures 9a and b, showed that while the surface layers have oxidized, some MoS<sub>2</sub> has remained in the deeper layers. Thus the layered structures are likely to provide the most effective encapsulation of the MoS<sub>2</sub> from oxidation. This approach of fabricating composite films were pursued further.

The microstructure of composite film #5 was analyzed by cross-section TEM. Figures 10a and b show the cross-section bright and dark-field micrographs of the composite film. A layered structure of the film consisting of crystalline and amorphous layers are clearly evident in these figures. The selected area diffraction (SAD) pattern of the film (Figure 11) was analyzed to identify the crystalline layers. The analysis is shown in Table 8.

The results presented in Table 8 clearly demonstrate that the crystalline layer is ZnO. The amorphous layer is composed of both MoS<sub>2</sub> and ZnO. The crystalline ZnO layer is highly textured. The vertical dimension of the crystallites is limited by the thickness of the layers, but the lateral dimension ranges from 30Å to 200Å. The layer thicknesses as determined from the cross-section micrographs are shown in Table 9.

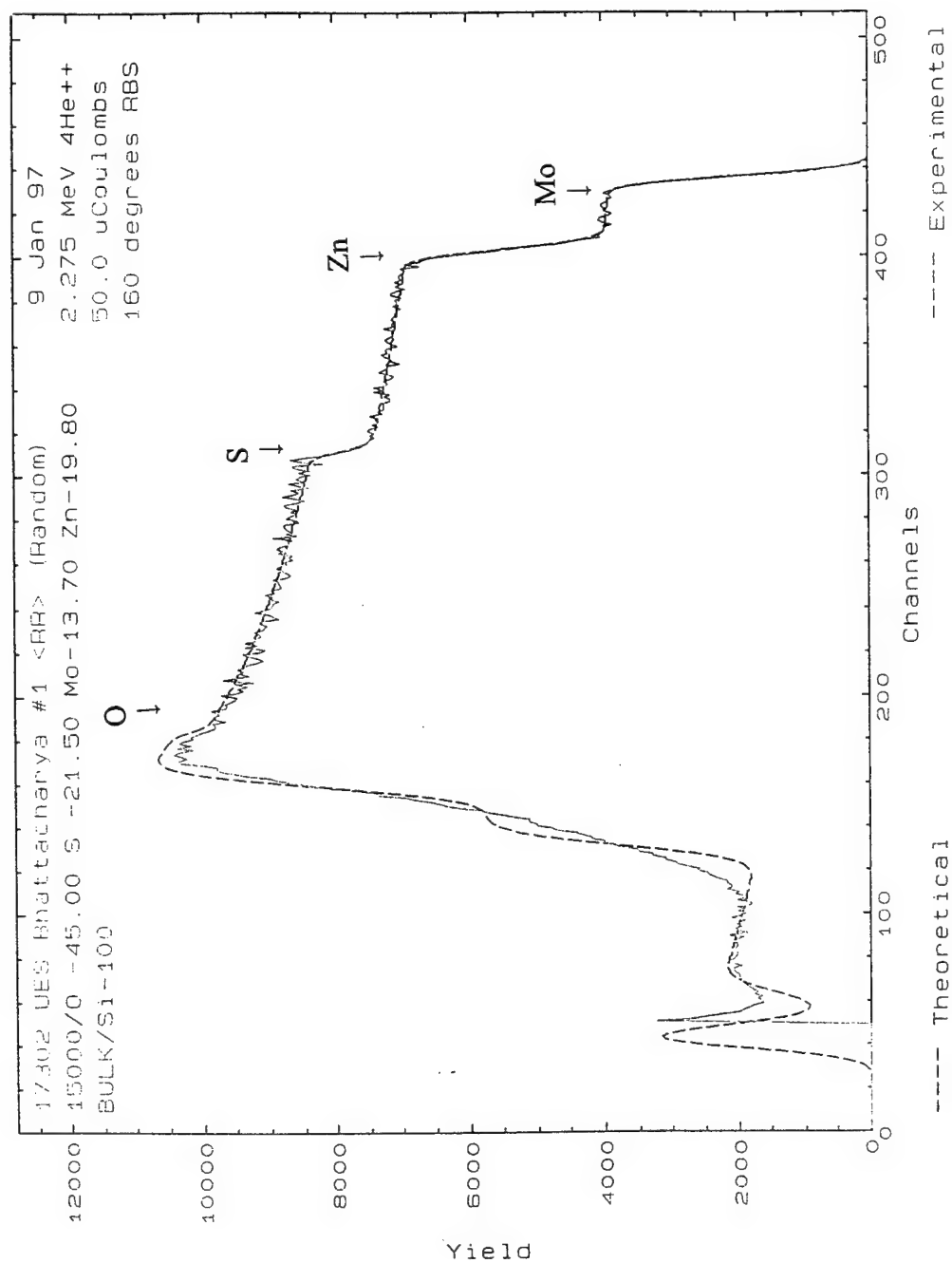


Figure 3. RBS Spectrum of Composite Film #1.

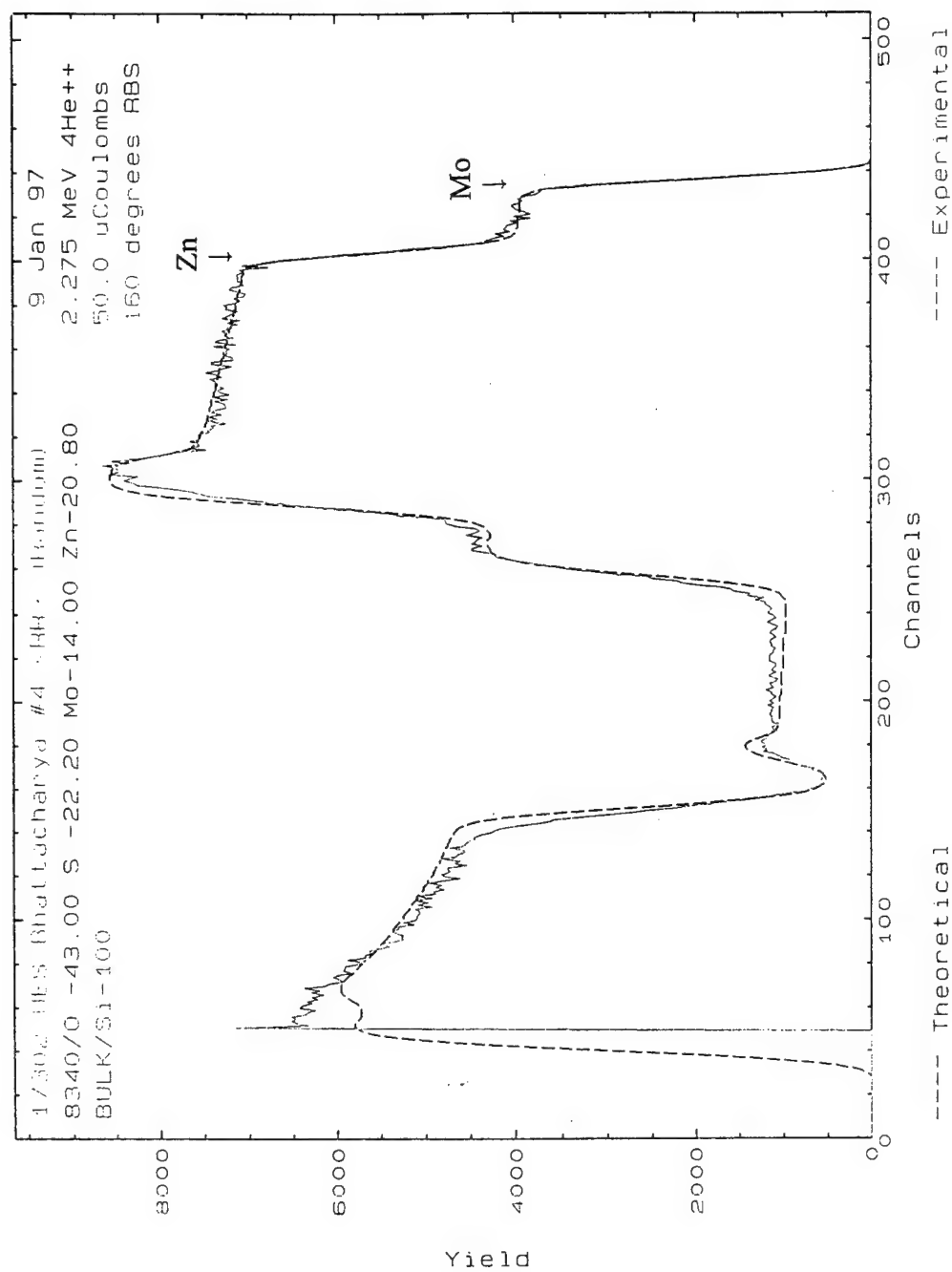


Figure 4. RBS Spectrum of Composite Film #2.

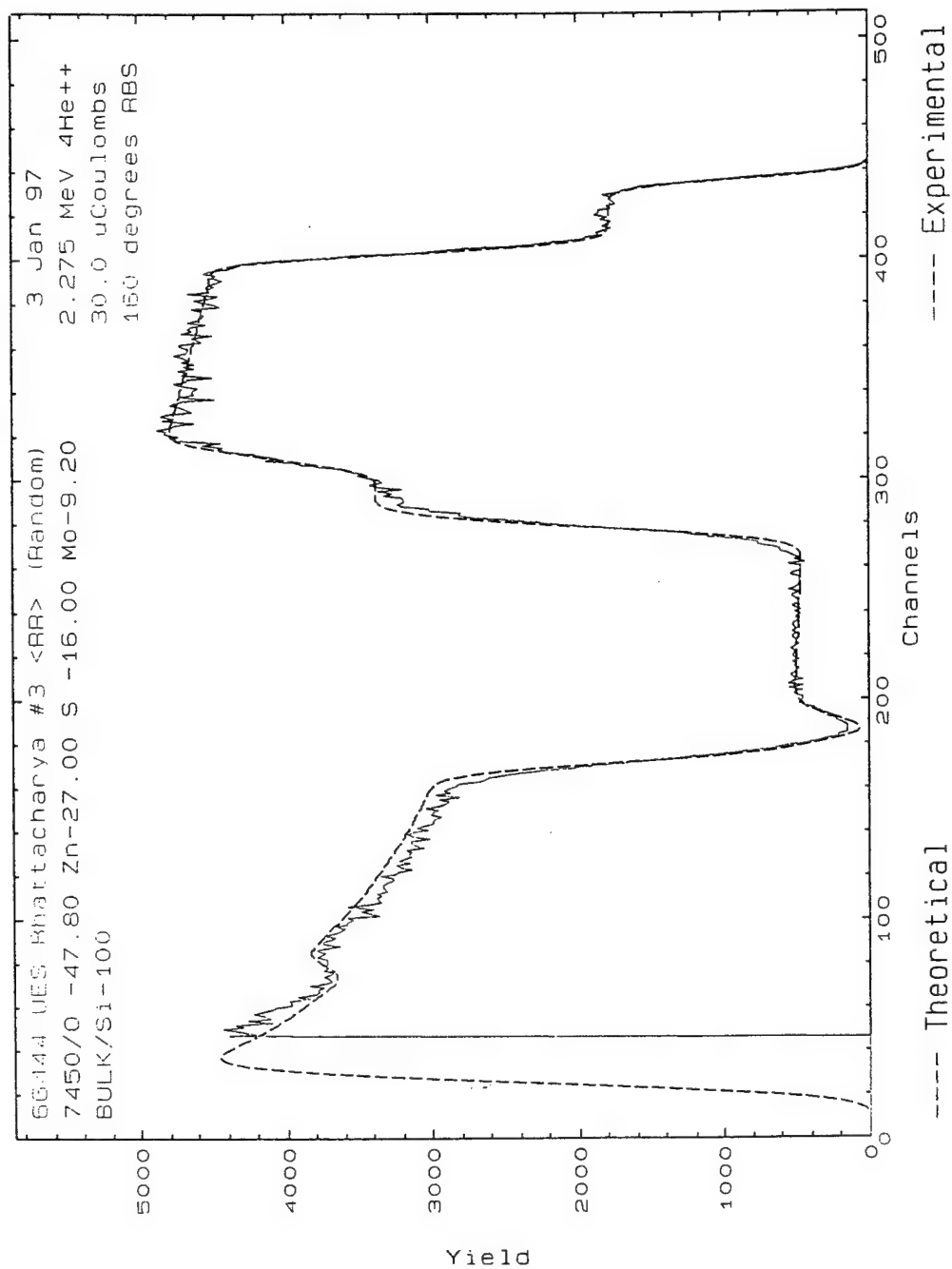


Figure 5. RBS Spectrum of Composite Film #3.

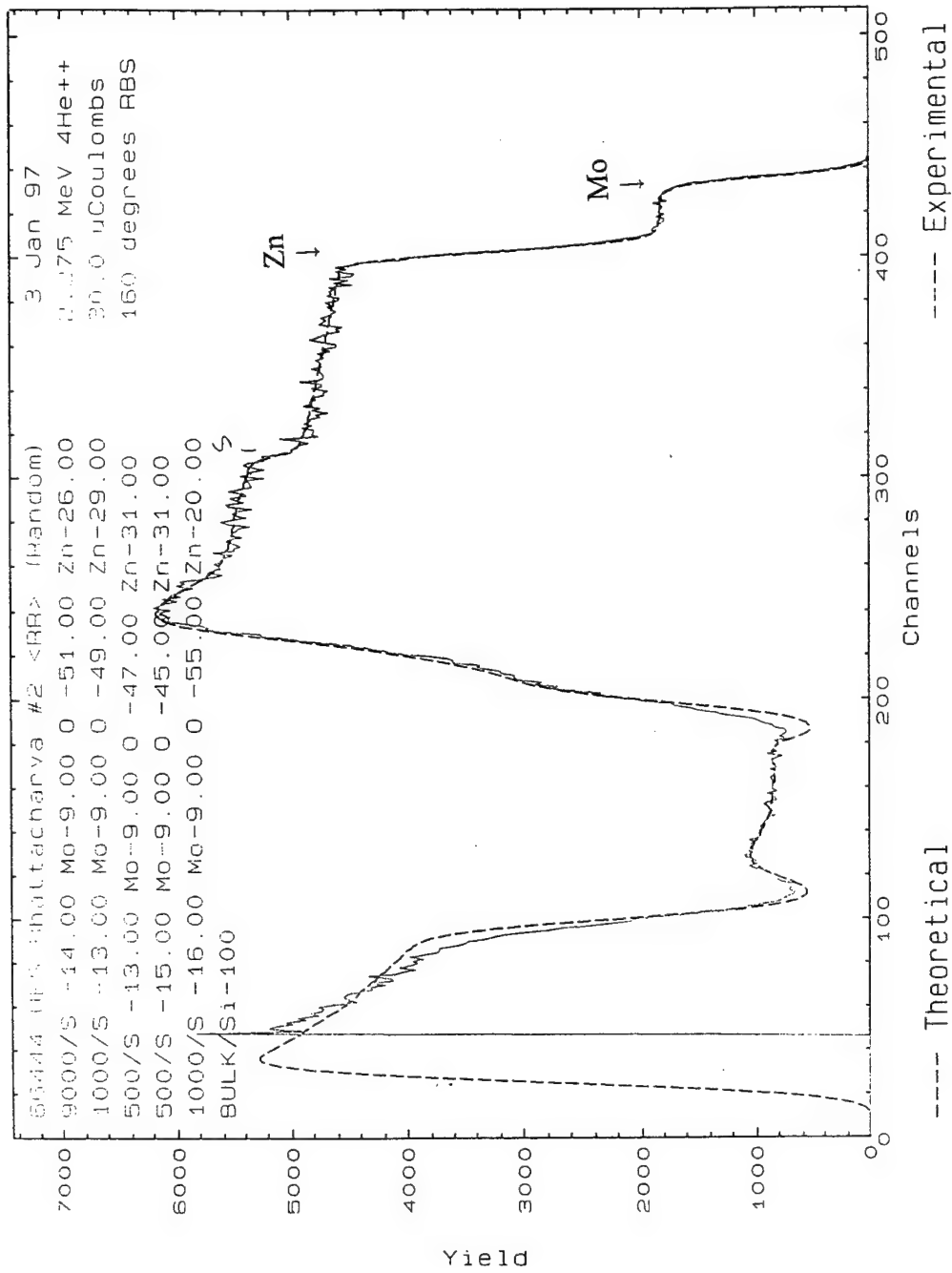


Figure 6. RBS Spectrum of Composite Film #4.

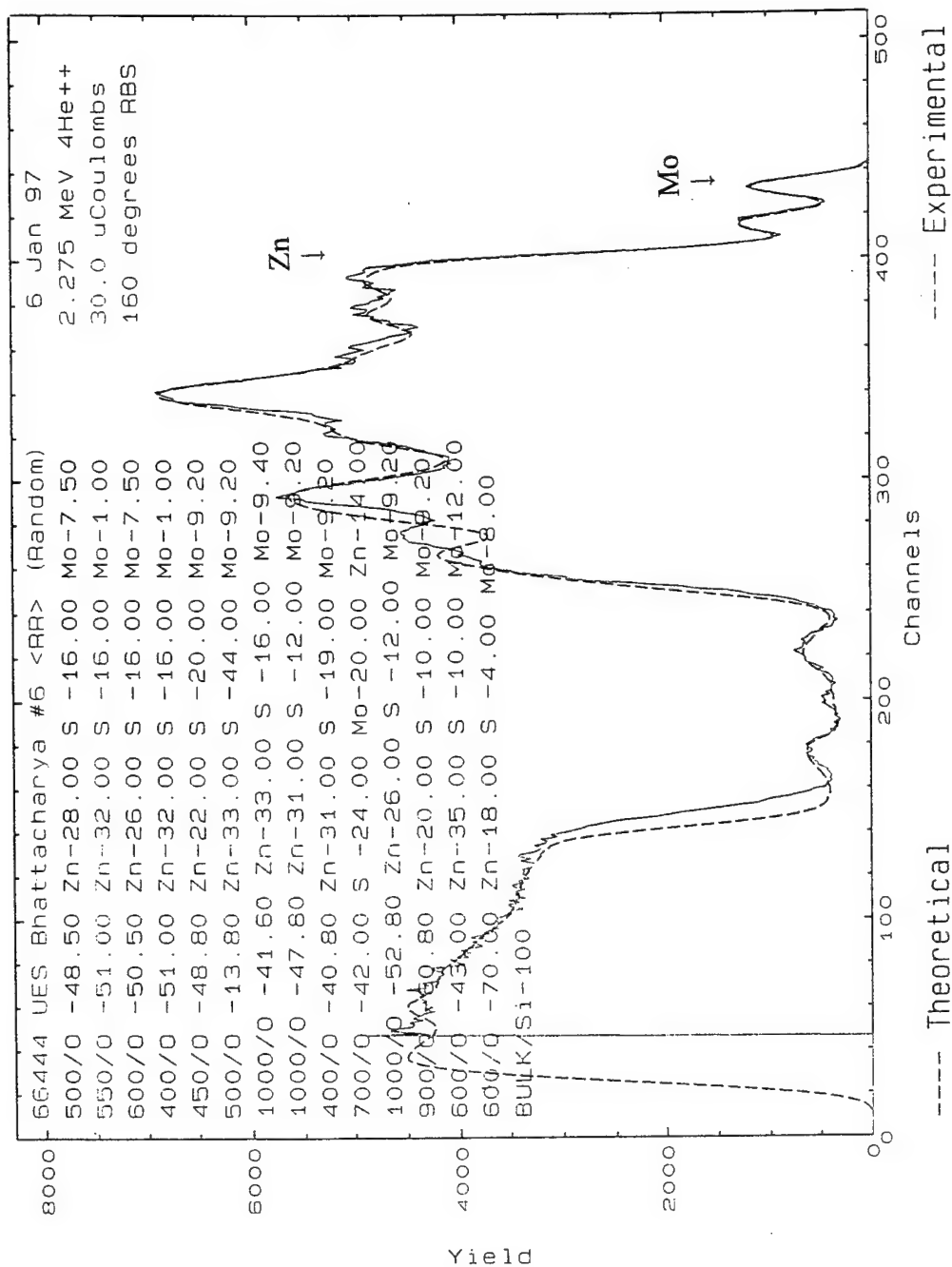


Figure 7. RBS Spectrum of Composite Film #5.

Table 3. Parameters for Theoretical Fit of the RBS Spectrum of Figure 3

Depth (Angstroms)	Atomic Concentration							Density*
	O	Si	S	Zn	Mo	S/Mo	O/Zn	
<15000	45.0	—	21.5	19.8	13.7	1.57	2.27	6.96E22
>15000	—	100	—	—	—	—	—	5.00E22

\*In units of atoms/cc

Table 4. Parameters for Theoretical Fit of the RBS Spectrum of Figure 4

Depth (Angstroms)	Atomic Concentration							Density*
	O	Si	S	Zn	Mo	S/Mo	O/Zn	
<8340	43.0	—	22.2	20.8	14.0	1.59	2.07	6.96E22
>8340	—	100	—	—	—	—	—	5.00E22

\*In units of atoms/cc

Table 5. Parameters for Theoretical Fit of the RBS Spectrum of Figure 5

Depth (Angstroms)	Atomic Concentration					Density(at/cc)
	O	Si	S	Zn	Mo	
<7450	45.0	—	21.5	19.8	13.7	6.94E22
>7450	—	100	—	—	—	5.00E22

Table 6. Parameters for Theoretical Fit of the RBS Spectrum of Figure 6

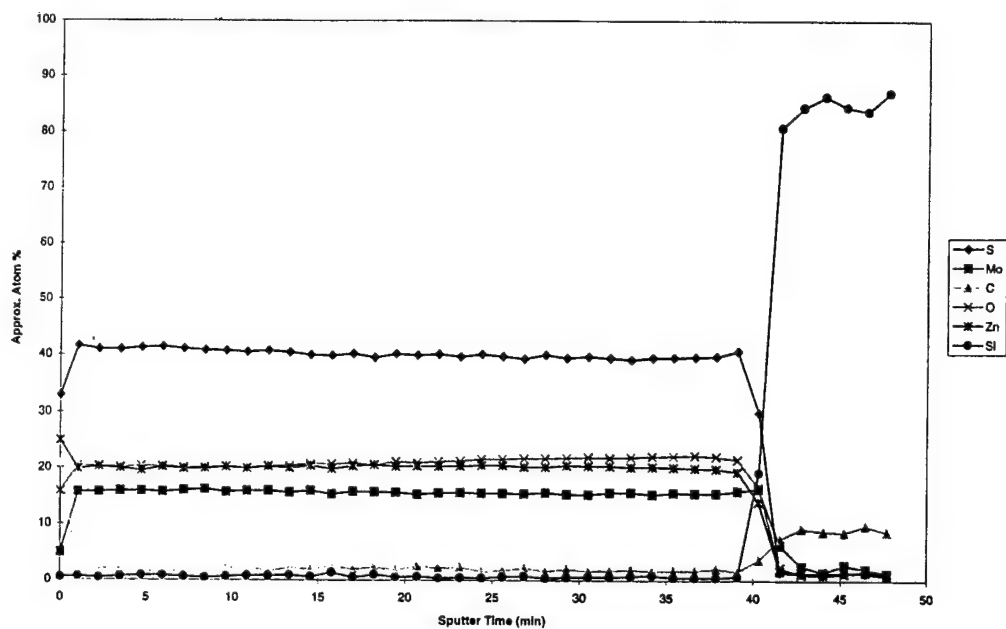
Depth (Angstroms)	Atomic Concentration					Density (at/cc)
	O	Si	S	Zn	Mo	
<9000	51.0	—	14.0	26.0	9.0	6.94E22
9000-10000	49.0	—	13.0	29.0	9.0	6.92E22
10000-10500	47.0	—	13.0	31.0	9.0	6.91E22
10500-11000	45.0	—	15.0	31.0	9.0	6.91E22
11000-12000	55.0	—	16.0	20.0	9.0	6.98E22
>12000	—	1000	—	—	—	5.00E22

Table 7. Parameters for Theoretical Fit of the RBS Spectrum of Figure 7

Depth (Angstroms)	Atomic Concentration							
	O	Si	S	Zn	Mo	S/Mo	O/Zn	Density*
<450	66.2	—	10.0	15.0	8.8	1.14	4.41	7.00E22
450-1000	60.0	—	—	40.0	—	—	1.50	6.89E22
1000-1650	29.0	—	20.0	43.0	8.0	2.50	0.67	6.86E22
1650-2150	63.0	—	—	37.0	—	—	1.70	6.91E22
2150-2650	18.0	—	34.0	33.0	15.0	2.27	0.55	6.91E22
2650-3350	63.0	—	—	37.0	—	—	1.70	6.91E22
3350-3850	32.0	—	40.0	20.0	8.0	5.0	1.60	7.04E22
3850-4350	60.0	—	—	40.0	—	—	1.50	6.89E22
4350-4650	20.0	—	40.0	20.0	20.0	2.00	1.00	6.96E22
4650-5150	55.0	—	—	45.0	—	—	1.22	6.86E22
5150-6250	37.0	—	25.0	18.0	20.0	1.25	2.06	6.93E22
6250-6650	50.0	—	10.0	40.0	—	—	1.25	6.91E22
6650-8350	44.0	—	10.0	36.0	10.0	1.00	1.22	6.87E22
8350-8750	65.0	—	3.0	32.0	—	—	2.03	6.94E22
>8750	—	100	—	—	—	—	—	5.00E22

\*In units of atoms/cc

(a)



(b)

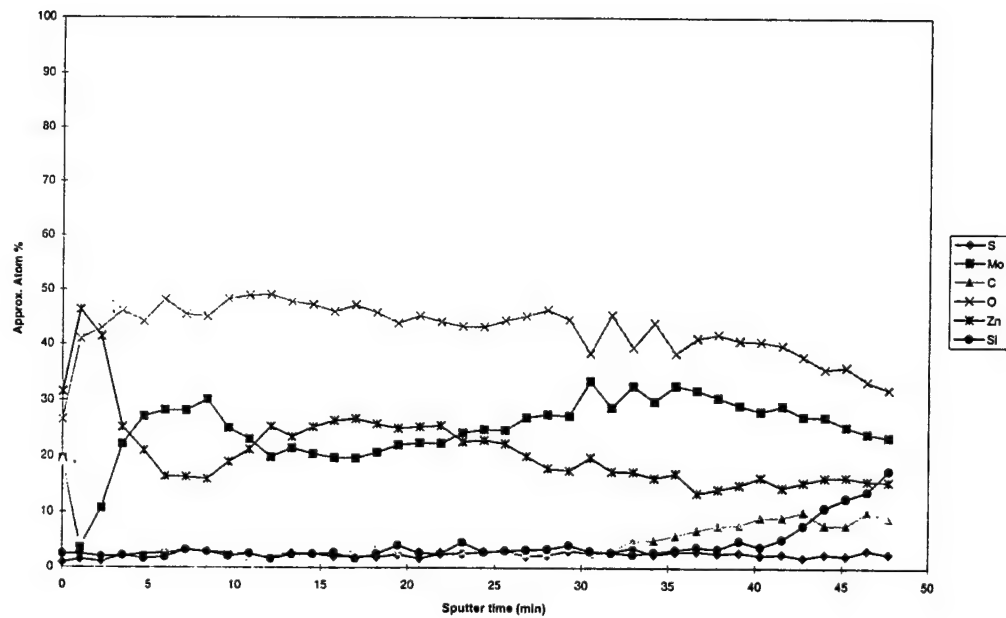
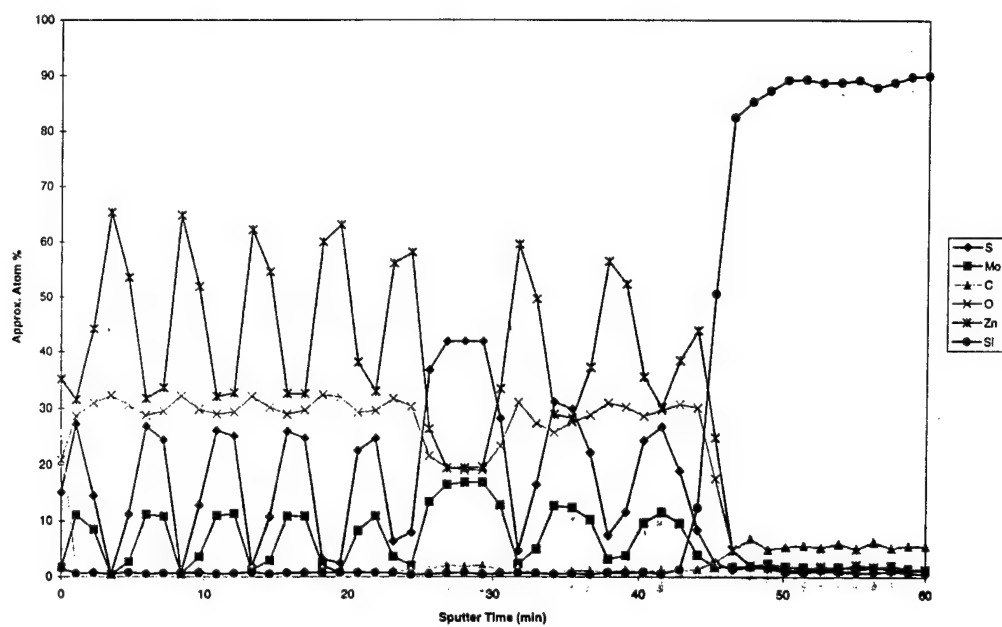


Figure 8. Auger Sputter Profiles of Sample #3, (a) As-deposited, (b) After Annealing at 600°C for 2 Hours.

(a)



(b)

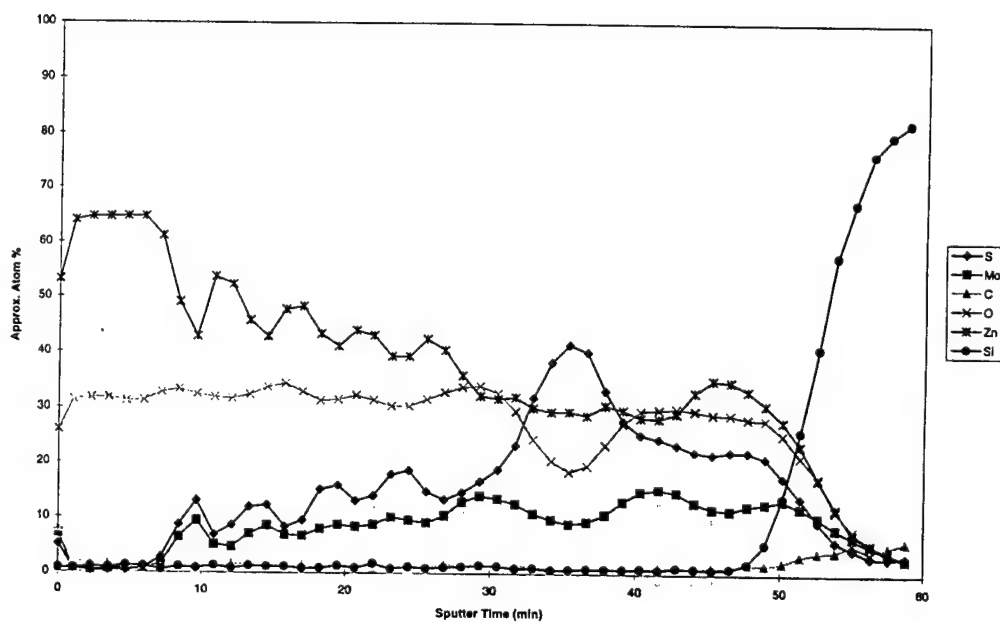


Figure 9. Auger Sputter Profiles of Sample #5, (a) As-deposited, (b) After Annealing at 600°C for 2 Hours.

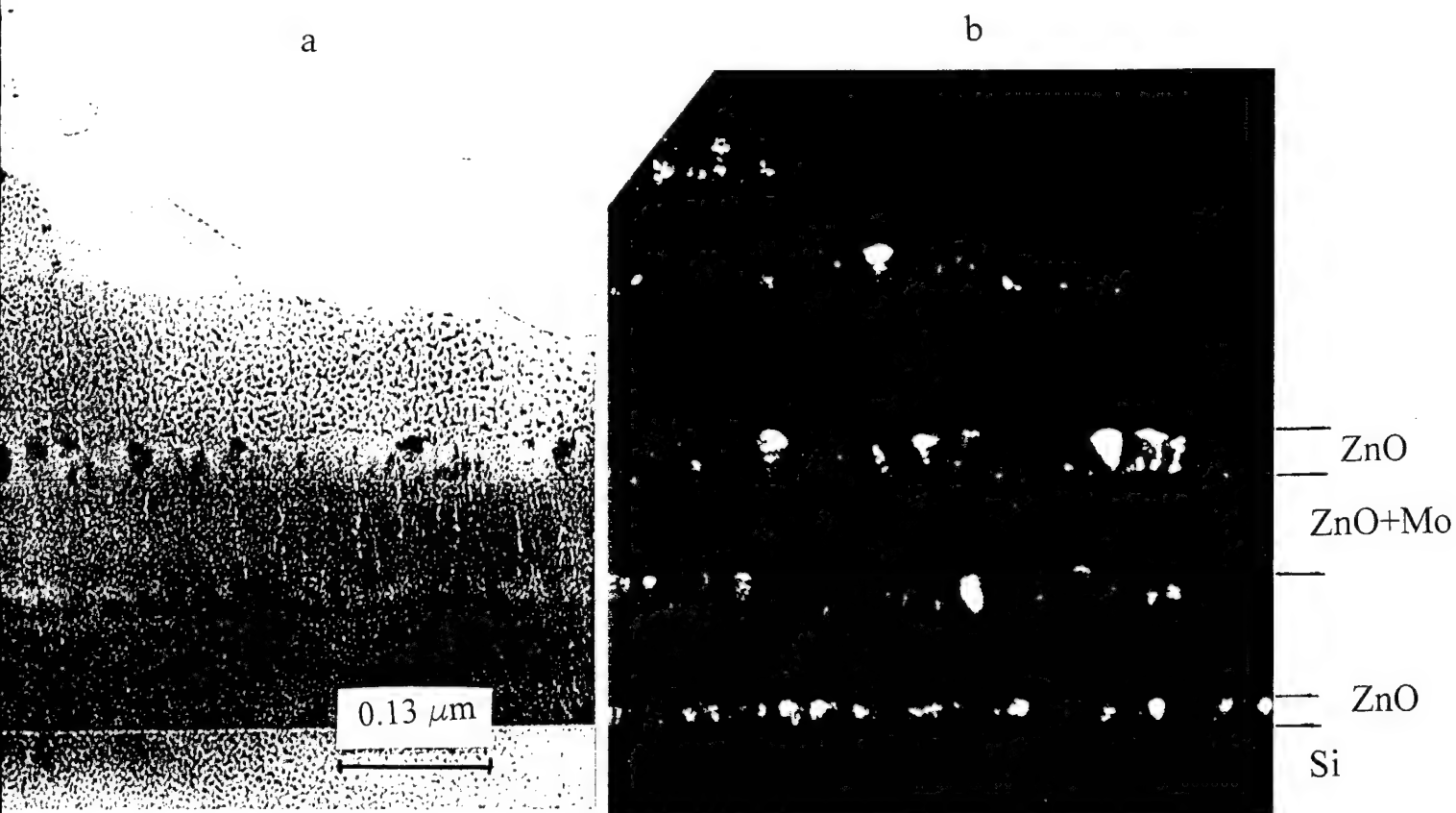


Figure 10. Cross-section Transmission Electron Micrographs of Composite Film #5, (a) Bright-field, (b) Dark-Field.

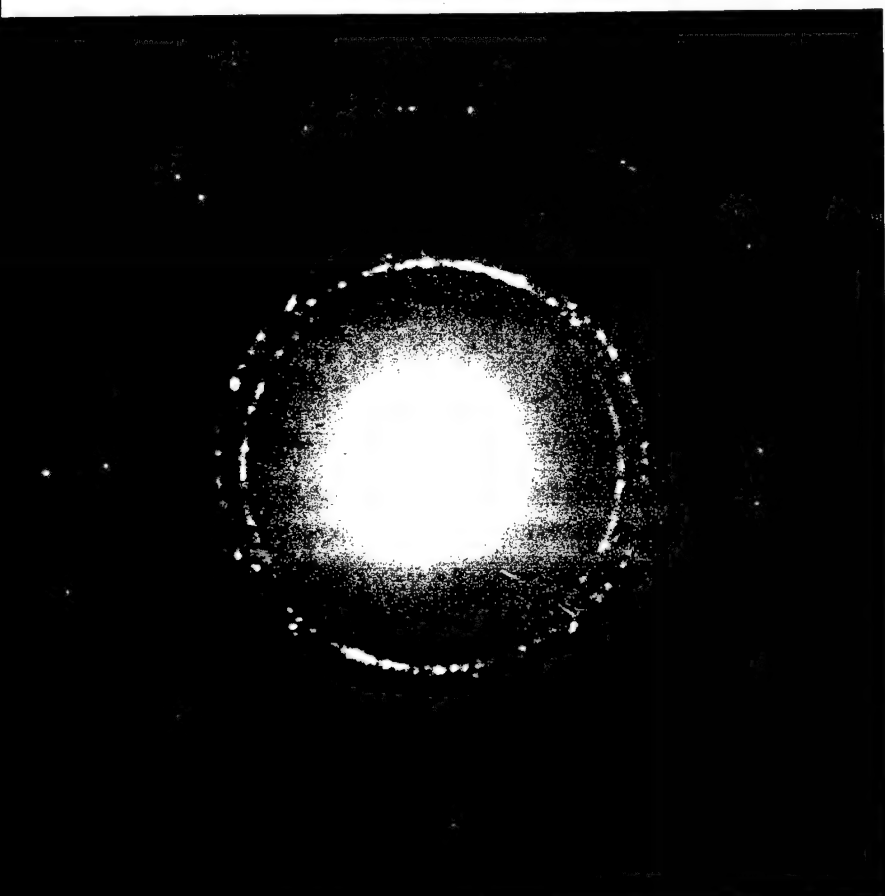


Figure 11. The Selected Area Diffraction Pattern of Composite Film #5.

Table 8. Observed d-values Compared to the Known d-values from X-ray Diffraction of Powders

Observed d-values (Å)	Known d-values (Å)	
	d (MoS <sub>2</sub> )	d (ZnO)
2.836	6.15	2.816
2.626	3.075	2.602
2.477	2.737	2.476
1.916	2.674	1.911
1.621	2.501	1.626
1.485	2.277	1.477
1.380	2.049	1.407
	1.830	1.319
	1.641	
	1.581	
	1.538	
	1.478	
	1.369	

Table 9. Layer Thicknesses

Layer No.	ZnO (Å)	ZnO+MoS <sub>2</sub> (Å)
1	200	
2		800
3	330	
4		850
5	430	
6		1270
7	400	
8		500
9	470	

### Optimization of Layered Structure

Based on the annealing results of layered structure where it was shown that some  $\text{MoS}_2$  was retained in the film even after annealing at  $600^\circ\text{C}$  for 2 hours in air, we have further optimized the layered structure. Overall  $\text{MoS}_2$  content in these new coatings deposited on  $\text{Si}_3\text{N}_4$  (sample #6) were reduced by reducing the  $\text{MoS}_2$  exposure of the substrate to 5 minutes at every 10 minutes interval. The AES sputter profiles of a representative coating on a  $\text{Si}_3\text{N}_4$  substrate is shown in Figure 12.  $\text{ZnO}$  layers are wider in the layered structure as compared to that in the previous deposition (Figure 8a). These samples were annealed at  $400^\circ\text{C}$ ,  $500^\circ\text{C}$  and  $600^\circ\text{C}$  for 1-3 hours in air. Annealing at  $400^\circ\text{C}$  for 1 hour did not produce any change in the layered structure. Some interdiffusion is evident after  $500^\circ\text{C}$ , 1 hour anneal, Figure 13a. The same sample was annealed again at  $600^\circ\text{C}$  for 1 hour. A few layers from the surface oxidized and S was lost, Figure 13b. The loss of S from the surface seems to be due to both inward and outward diffusion. However, extending the annealing to 3 hours at  $600^\circ\text{C}$ , resulted in the complete oxidation of the coating and total loss of S, Figure 13c.

## **4.2 FRICTION TEST RESULTS**

The results of the friction tests of  $\text{ZnO}+\text{MoS}_2$  films #1 - #5 on M50 substrates are shown in Figures 14-18. The results are shown for room temperature and  $400^\circ\text{C}$  only since the films delaminated at  $600^\circ\text{C}$  on M50 substrates. The friction coefficient is about 0.2 at room temperature for all of the samples. The initial friction coefficient at  $400^\circ\text{C}$  varied from 0.15 to 0.3 for all films except #3 that showed higher friction coefficient  $\sim 0.45$  in the beginning and rising quickly to 0.75. This indicated that the film came off upon contact with the ball. In most of these tests the coatings did not last very long indicating poor adherence to the substrates. This is not surprising since no attempts were made to improve the adherence by plasma cleaning of the substrate prior to deposition or ion bombardment during the deposition by appropriate biasing of the substrate.

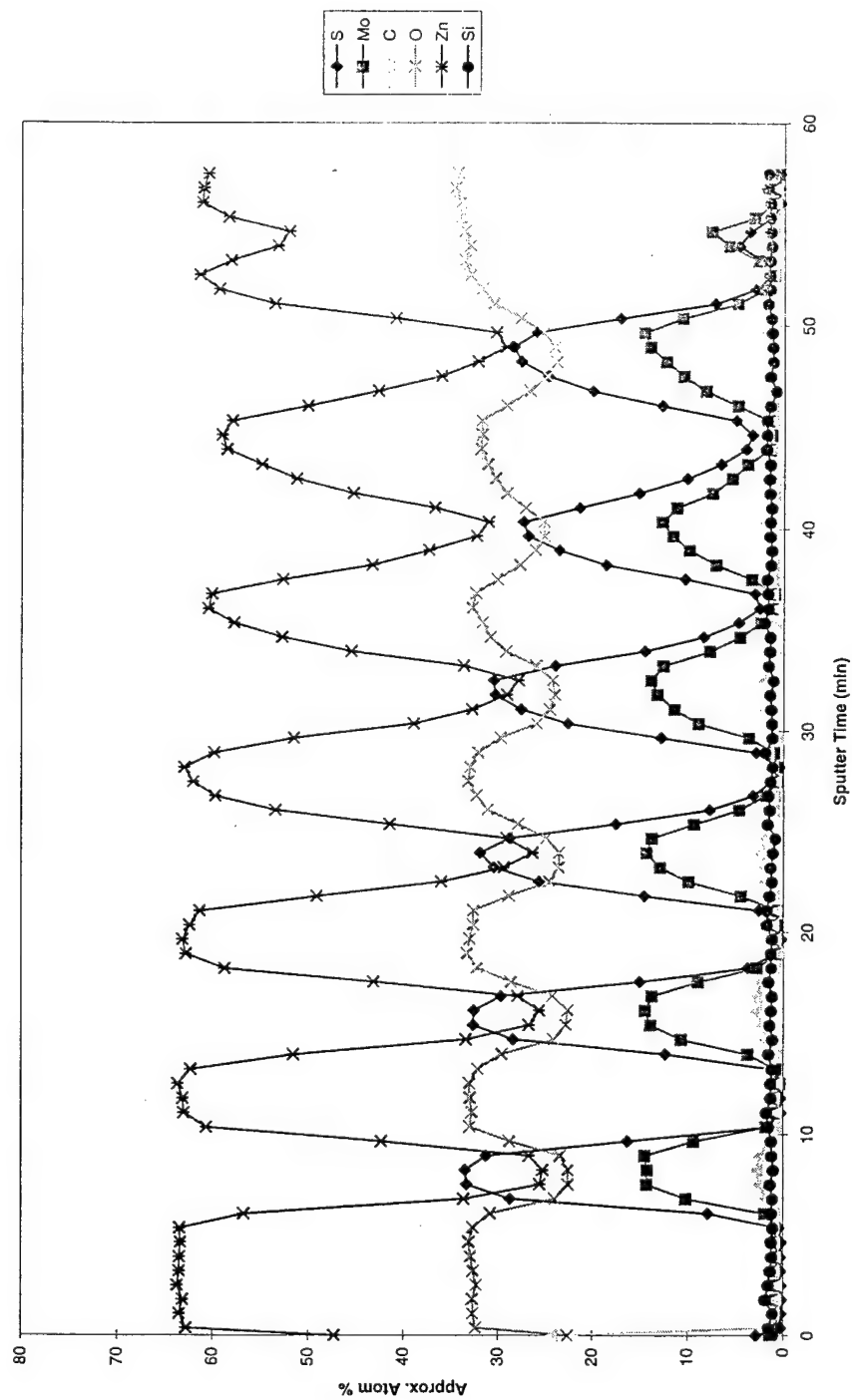


Figure 12. Auger Sputter Profiles of Sample #6, As-deposited.

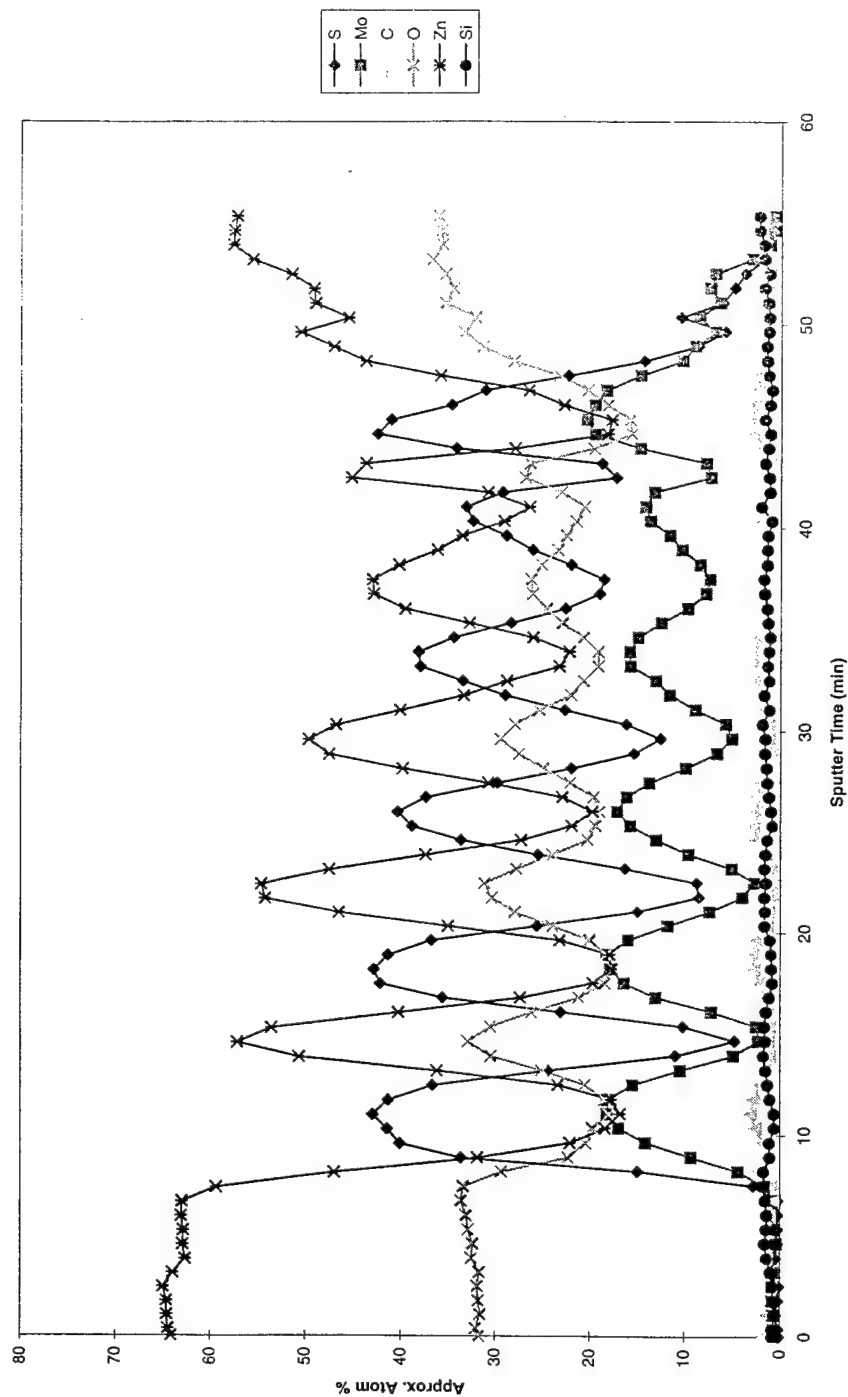


Figure 13a. Auger Sputter Profiles of Sample #6, After Annealing, 500°C, 1 Hour.

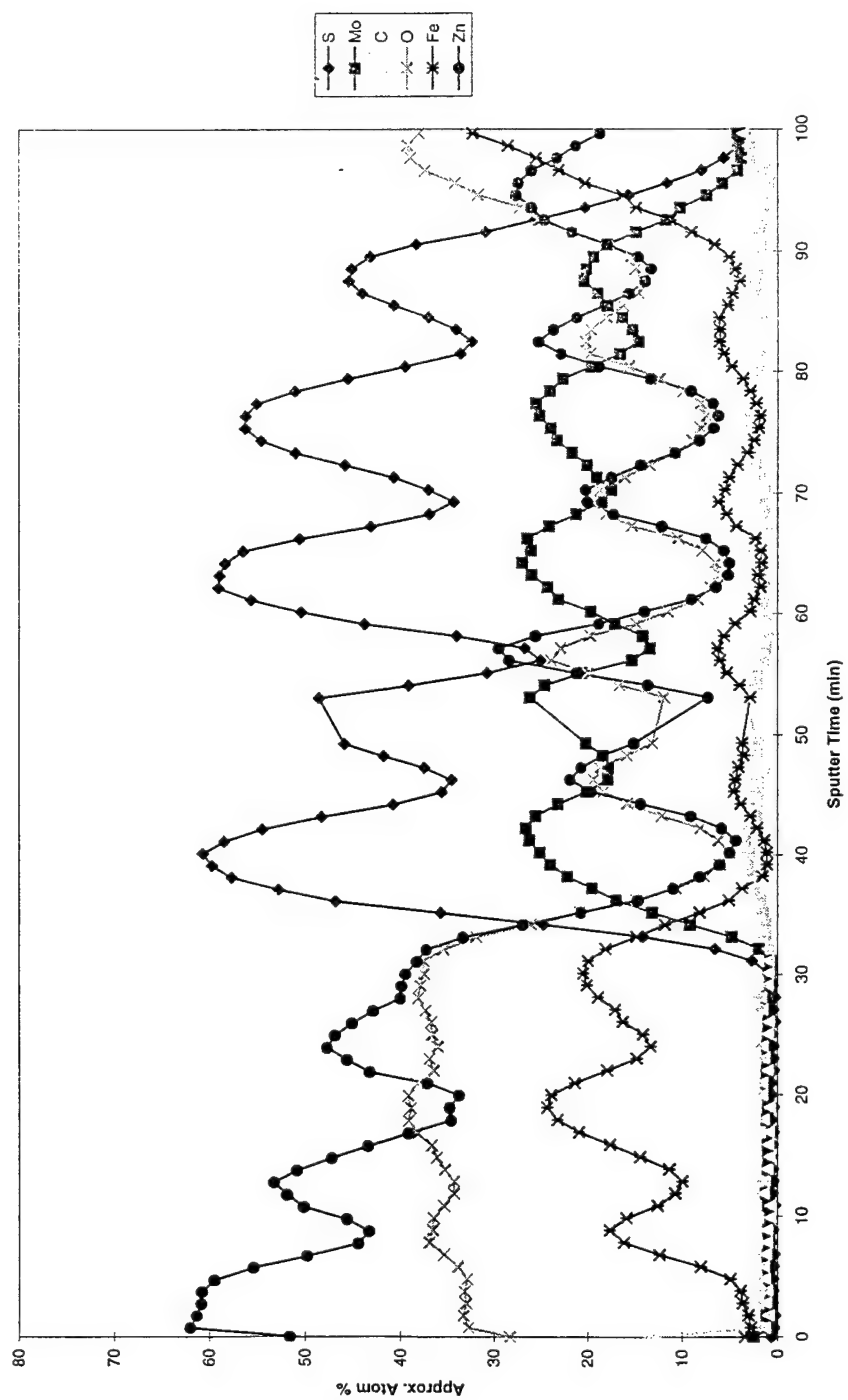


Figure 13b. Auger Sputter Profiles of Sample #6, After Annealing, 600°C, 1 Hour.

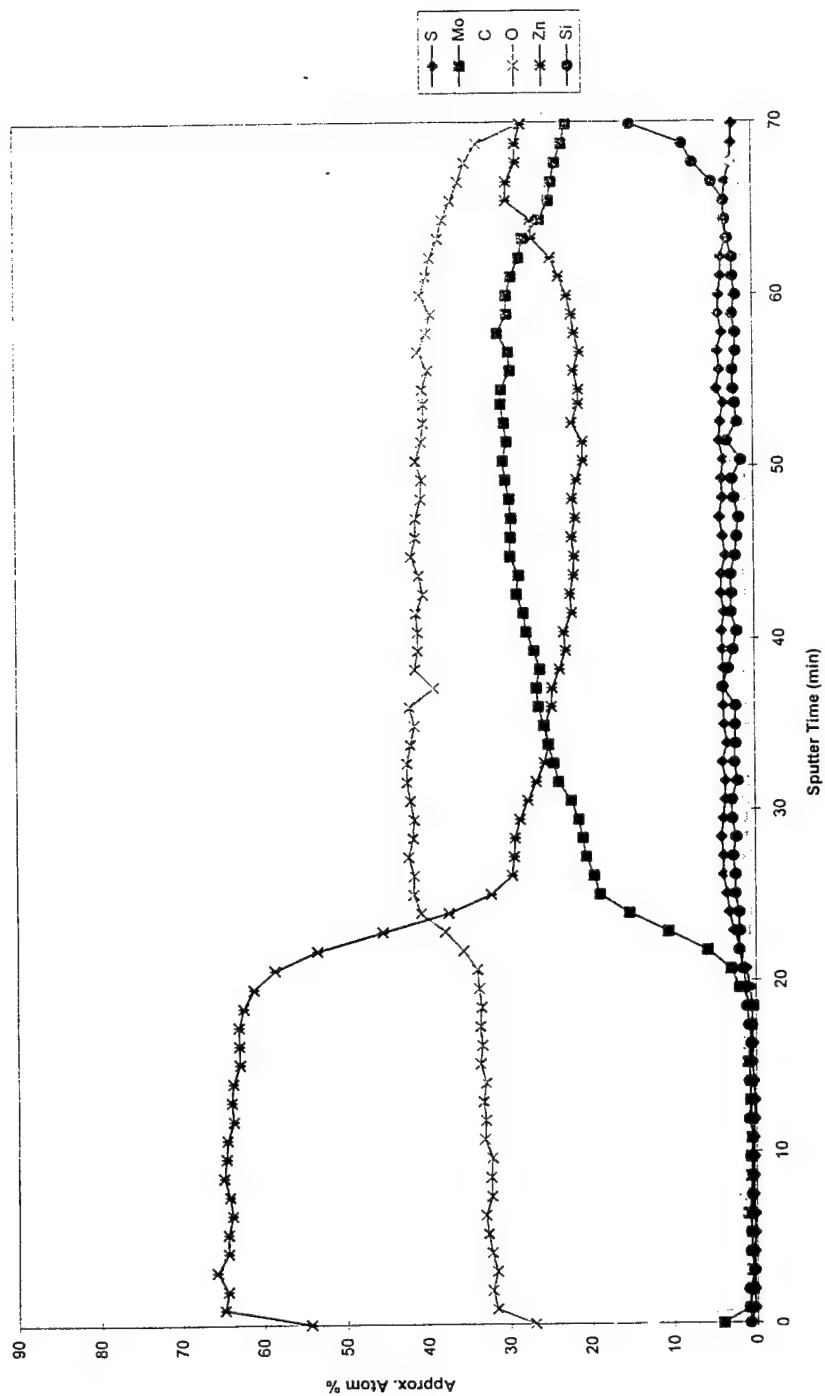


Figure 13c. Auger Sputter Profiles of Sample #6, After Annealing, 600°C, 3 Hours.

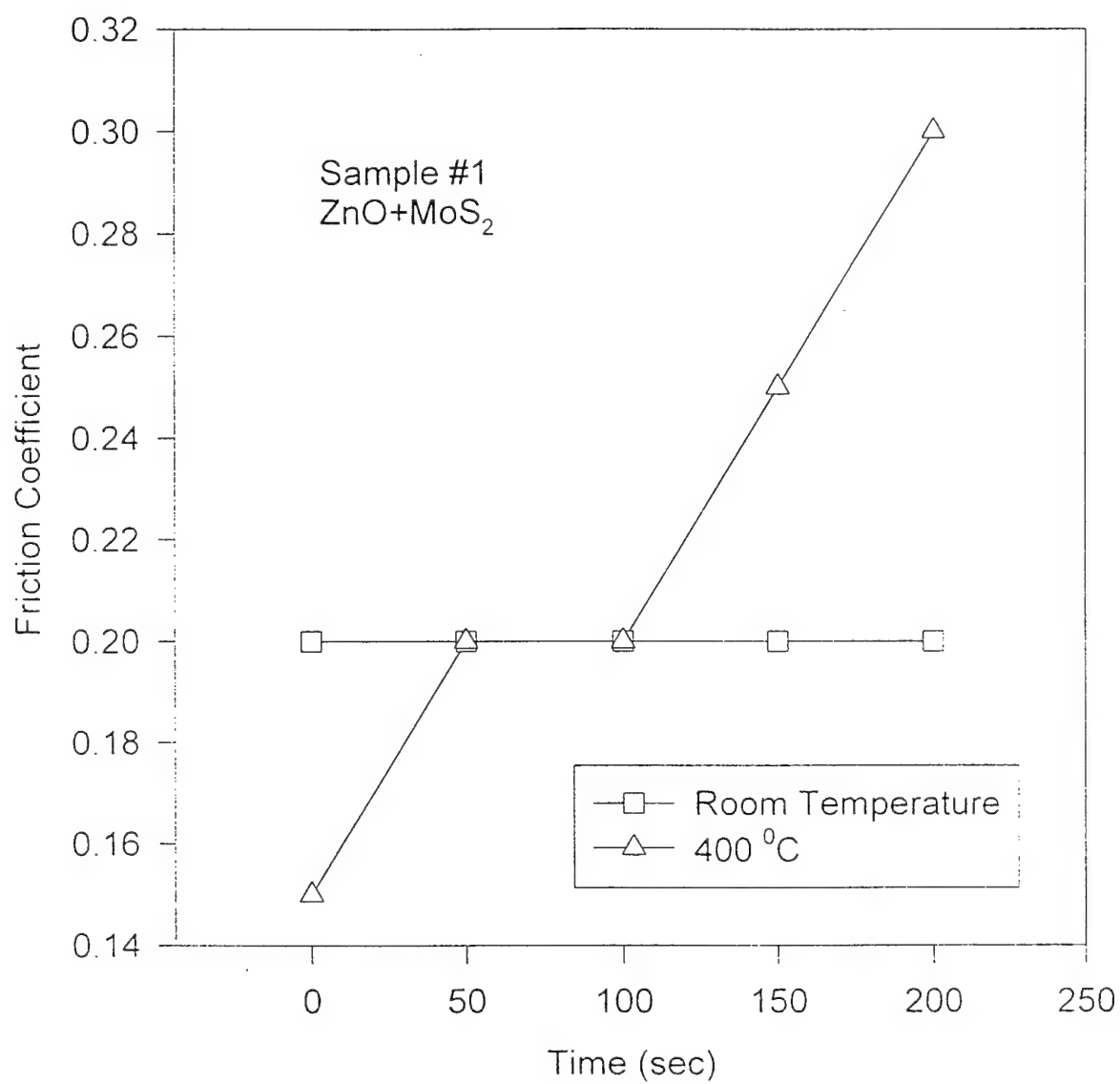


Figure 14. Friction Coefficient as a Function of Time for Sample #1.

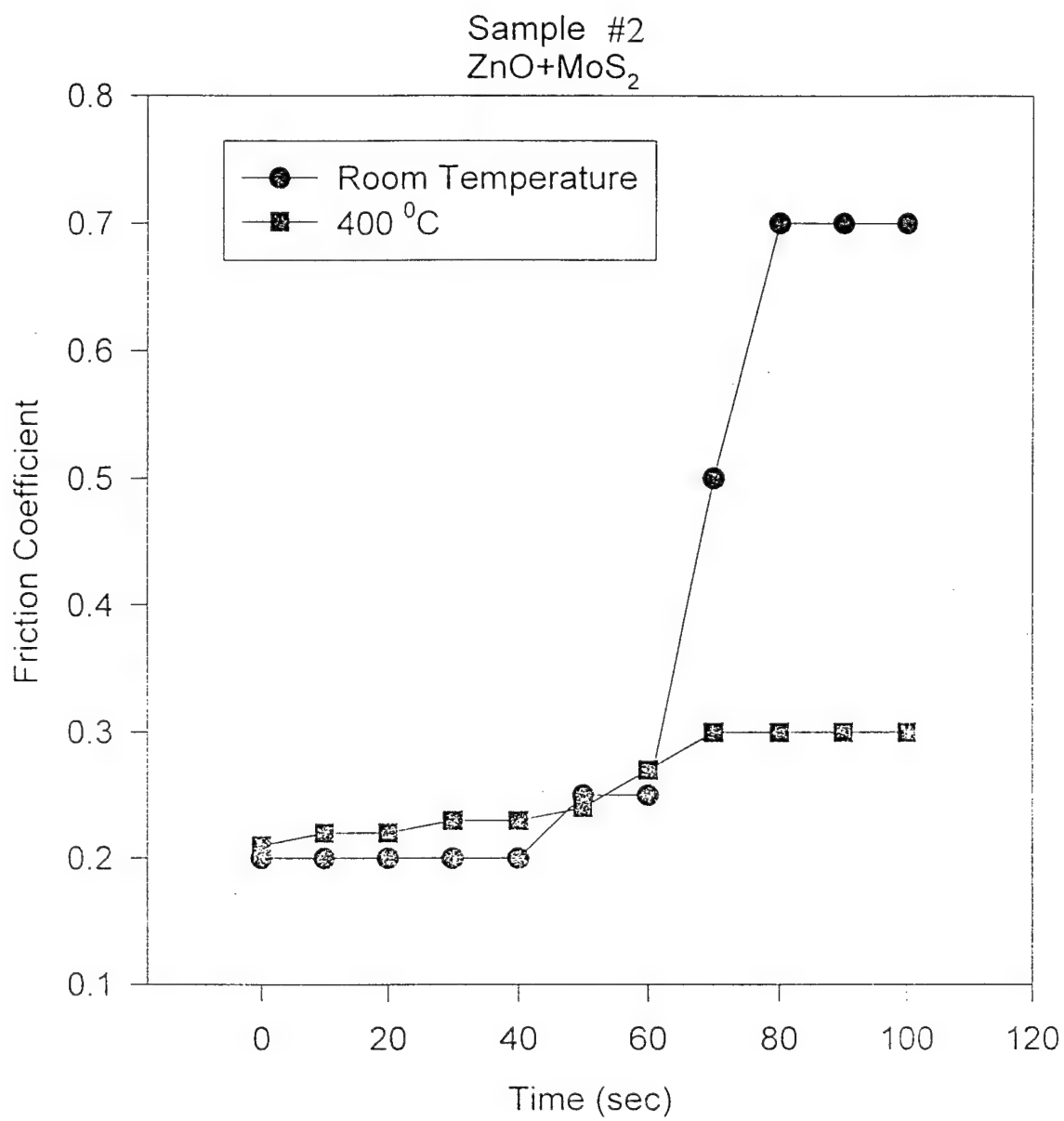


Figure 15. Friction Coefficient as a Function of Time for Sample #2.

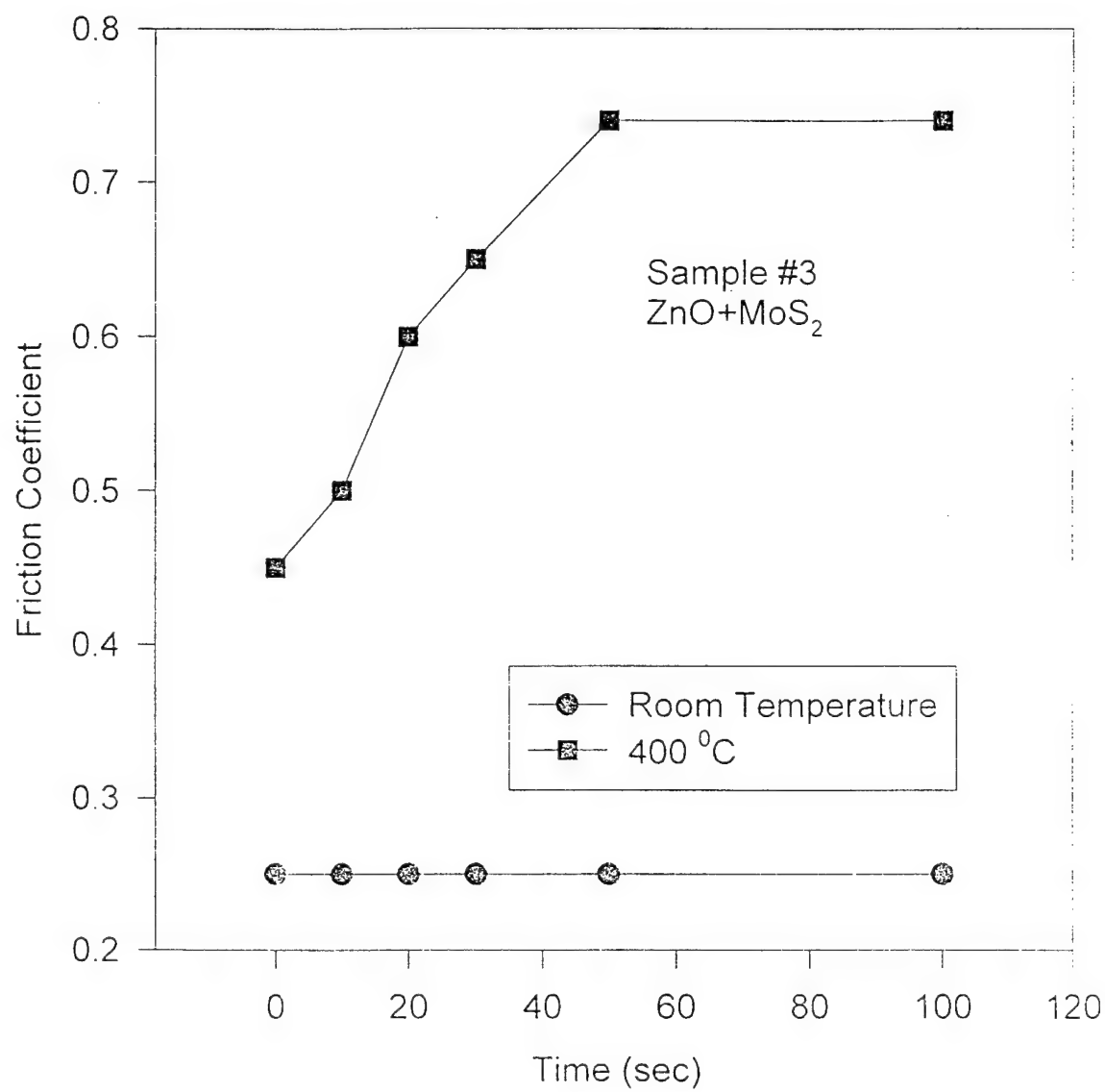


Figure 16. Friction Coefficient as a Function of Time for Sample #3.

Sample #4  
ZnO+MoS<sub>2</sub>

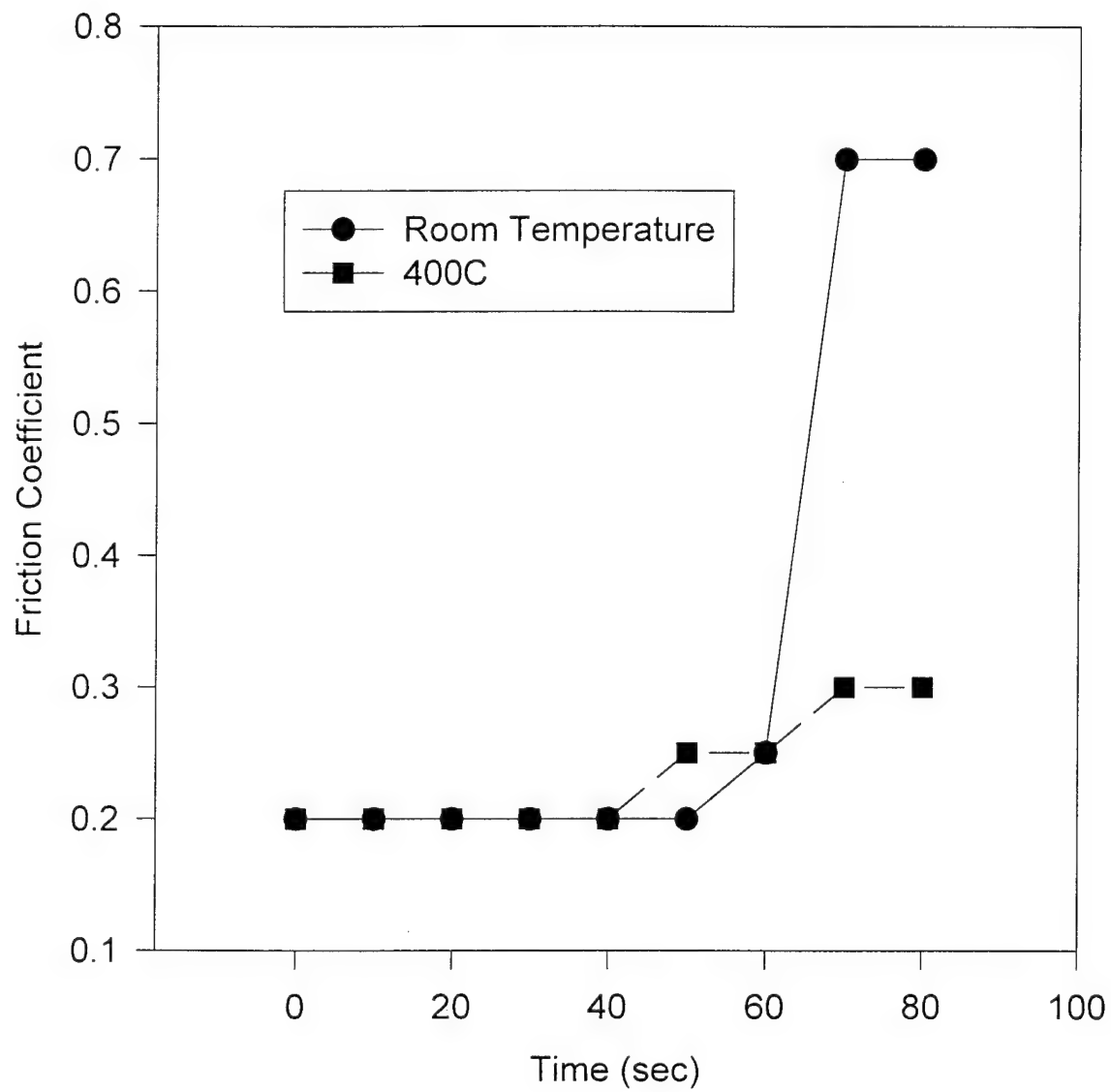


Figure 17. Friction Coefficient as a Function of Time for Sample #4.

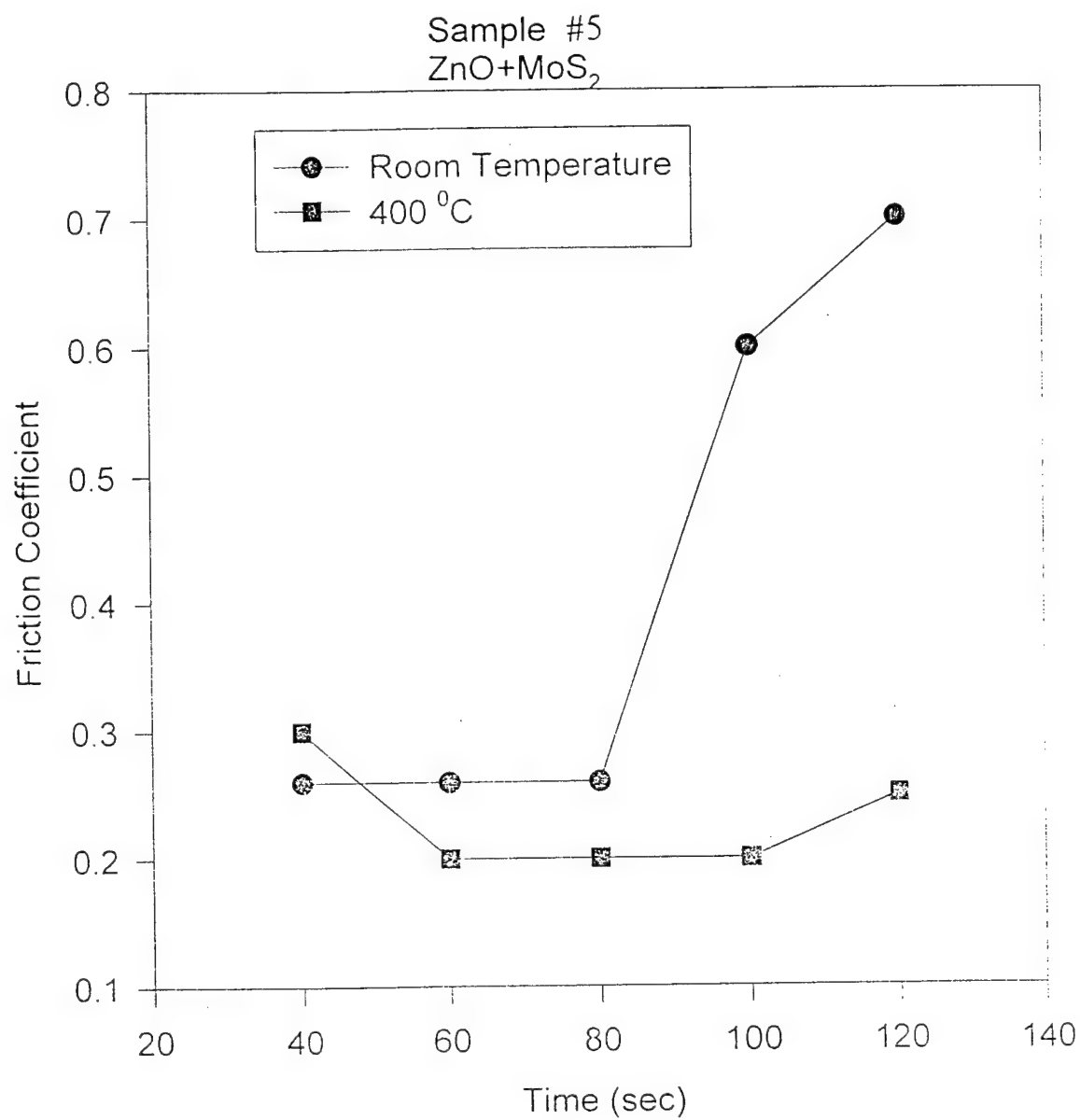


Figure 18. Friction Coefficient as a Function of Time for Sample #5.

Friction tests at higher temperatures, 500°C-700°C, were performed by using sample #6 on Si<sub>3</sub>N<sub>4</sub> substrate. Figure 19 shows the plot of friction coefficient as a function of time for sample #6 at 500°C, 600°C and 700°C. Friction coefficients were low, ~0.4 at 600°C and 700°C. However, it started higher, ~0.70, at 500°C and then dropped to <0.4 after the surface layers worn off. This is due to the fact that at 500°C annealed sample, the surface layer is ZnO which produces higher friction. Lower friction after a certain period of time is indicative of exposure of the contact region to underlying MoS<sub>2</sub>. The lower friction coefficient at 600°C and 700°C may be due to the formation of zinc molybdates.

### 4.3 DISCUSSION OF RESULTS

In view of the results presented thus far, one may ask the following questions: (1) what are the friction coefficients of ZnO and MoS<sub>2</sub> at elevated temperatures in air? (2) What is the friction coefficient of the M50 sliding on M50 at elevated temperatures in air? In order to answer these questions we have performed a few tests using ZnO and MoS<sub>2</sub> films. The results are shown in Figures 20 and 21. At room temperature, the friction coefficient of ZnO is rather low, ~0.25, that increases to ~0.3 in 100 sec of run time. But at 400°C and 600°C, the friction coefficient starts at about 0.6, staying at that level (400°C) or slightly decreasing to about 0.5 in 100 sec (600°C). MoS<sub>2</sub> has shown a low friction, 0.06-0.15, up to 300°C as expected. At 400°C the friction coefficient rapidly increased from about 0.27 to 0.45 in 100 sec. The friction coefficient of M50 on M50 is about 0.7 at room temperature that decreases to 0.4 at 400-600°C. Based on these results, the friction coefficient of 0.2-0.3 for ZnO+MoS<sub>2</sub> films at room temperature (Figures 14-18) can be explained to be due to both the constituents, i.e., ZnO and MoS<sub>2</sub>. At 400°C, the friction coefficient of ZnO+MoS<sub>2</sub> is mainly due to the presence of MoS<sub>2</sub>. The mixed composite films have delaminated at higher temperature (~600°C), particularly on M50 substrates. This is primarily due to the escape of S as SO<sub>2</sub> during annealing that weakened the interfacial bond between the film and the substrate. To verify it further, we looked at the surface of sample #5 after the friction tests at 400°C under an optical microscope (Figure 22). The presence of bubbles clearly indicate the evolution of gas, thus supporting this hypothesis. At higher temperature, more bubbles are formed that eventually burst thus exfoliating the film.

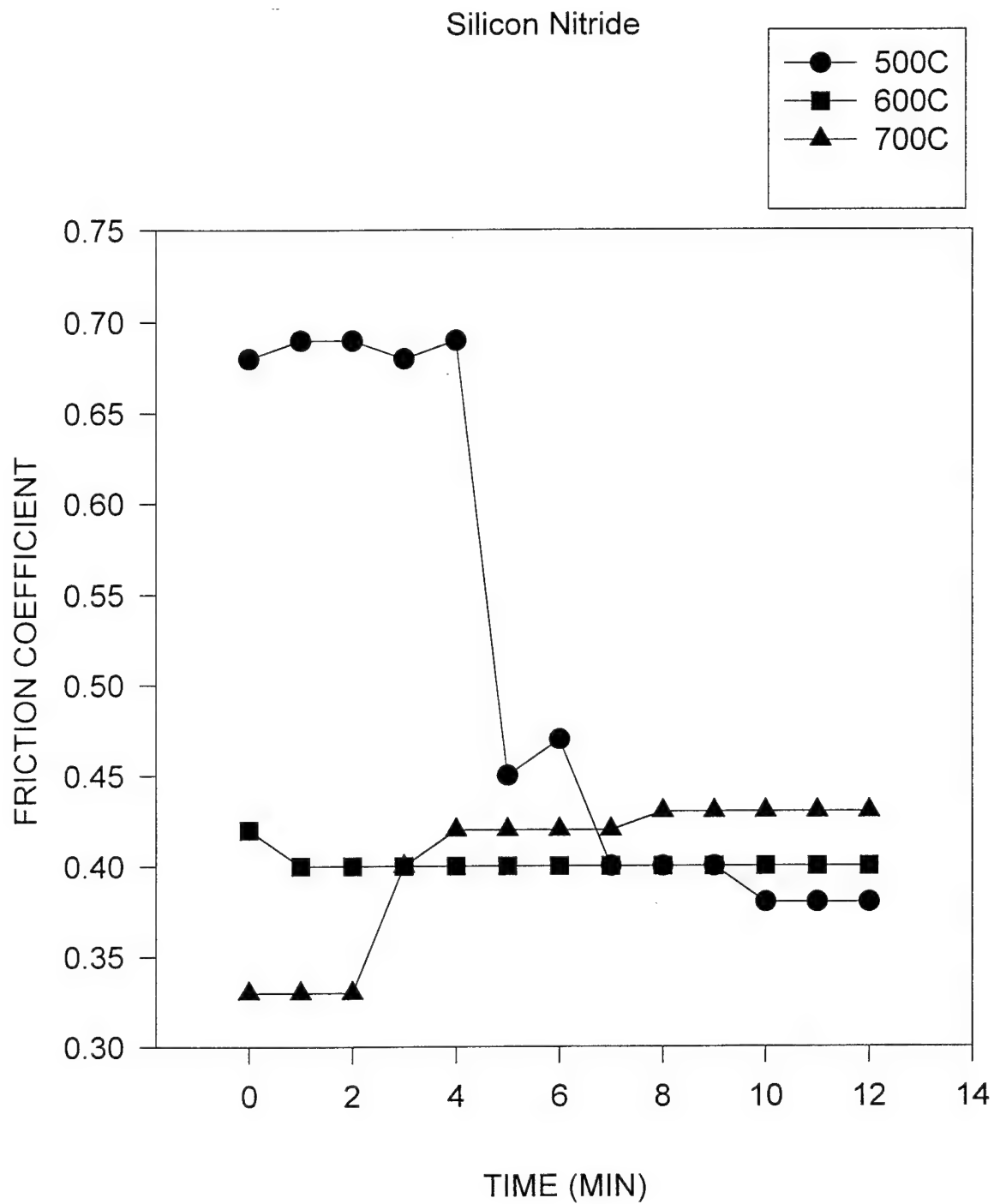


Figure 19. Friction Coefficient as a Function of Time for Sample #6.

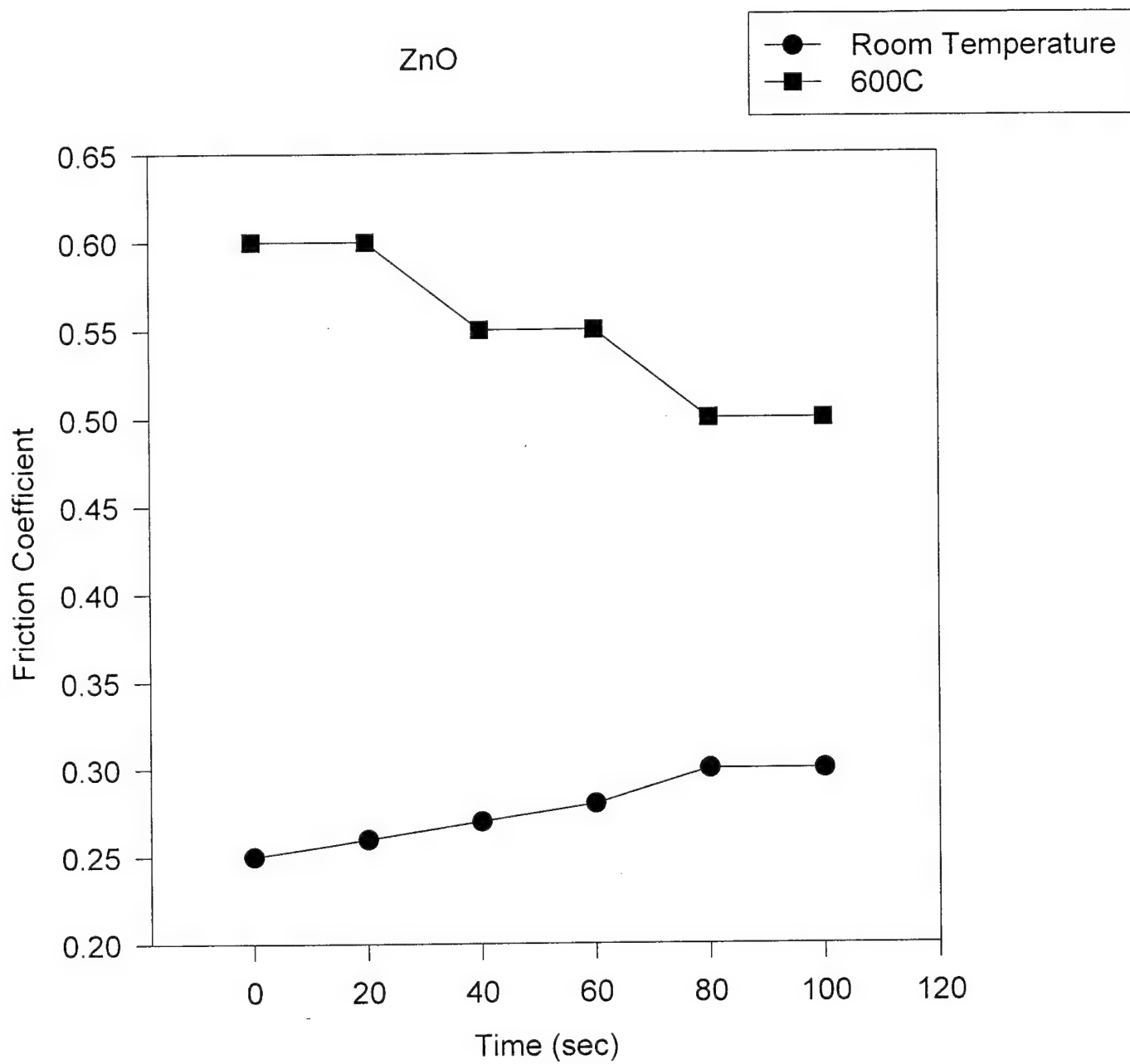


Figure 20. Friction Coefficient as a Function of Time for ZnO Film on M50.

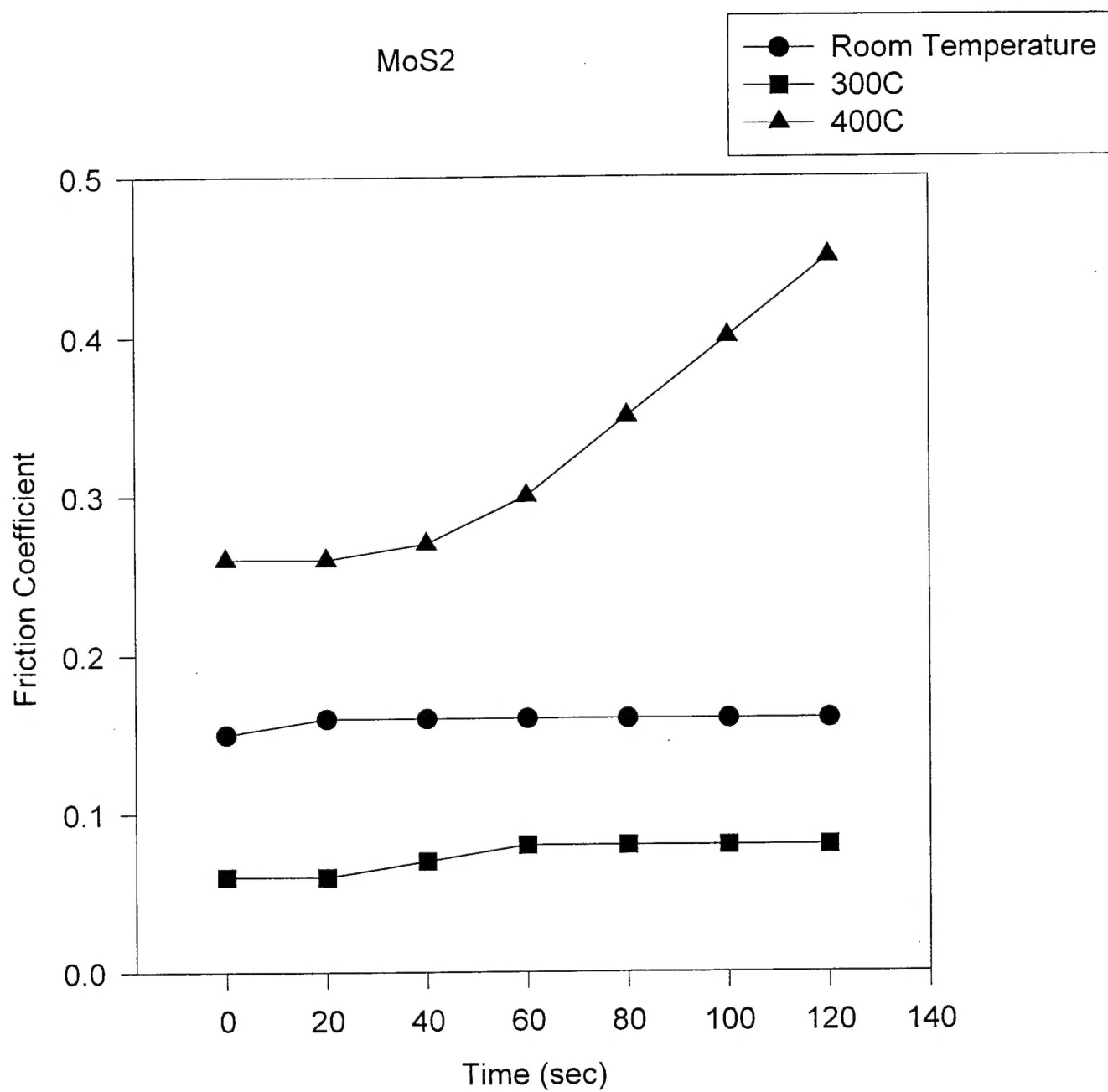


Figure 21. Friction Coefficient as a Function of Time for MoS<sub>2</sub> Film on M50.

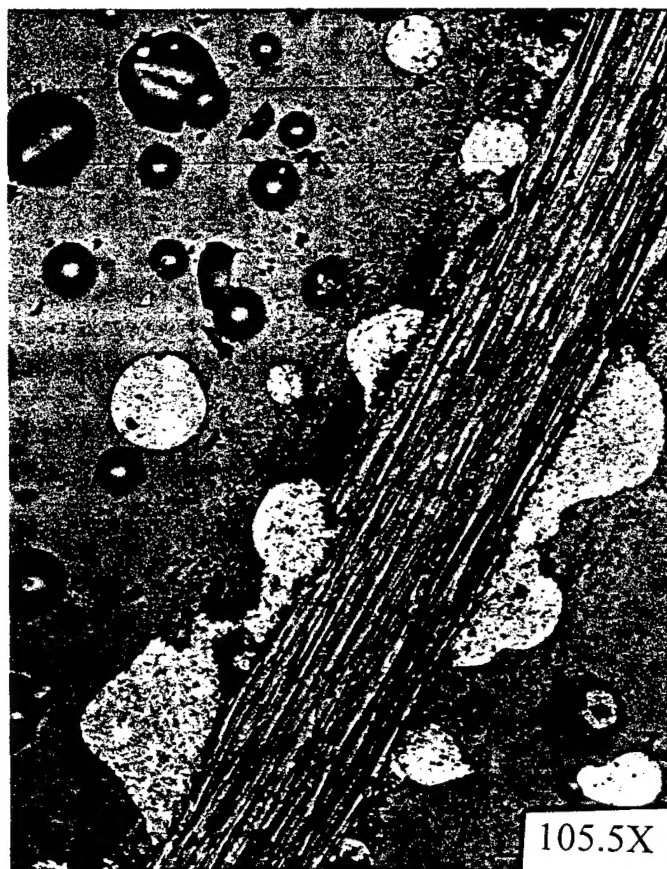


Figure 22. Optical Micrograph of the Sample #5 After Friction Tests at 400°C.

Layered composite films on  $\text{Si}_3\text{N}_4$  after annealing at  $600^\circ\text{C}$  remained intact even after annealing for 3 hours. The friction coefficients were higher because of oxidation of  $\text{MoS}_2$ . Thus, it can be concluded that  $\text{ZnO}$  did not act as an effective barrier to oxidation at temperatures above  $500^\circ\text{C}$ .

## 5.0 POTENTIAL APPLICATIONS

Solid lubricant coatings are extensively used in spacecraft. Launch vehicles and spacecraft have various release mechanisms that permit the spacecraft to separate from the launch vehicle. Spacecraft also have deployment mechanisms that allow subsystems (e.g., antenna dishes, solar panels), which are often folded during launch to conserve volume, to be opened in orbit. These release or deployment mechanisms require a lubricant to provide low friction (torque) for a low number of cycles. Lack of thermal control may require the lubricant to function in a wide temperature range. The coatings developed in Phase I, after further optimization in Phase II, may be applied on spacecraft mechanisms.

Also, solid lubricant coatings developed in Phase I can be used in metals and ceramics bearing for high temperature,  $\approx 500^\circ\text{C}$ , applications. Ceramics are being considered for gas turbine engine applications such as in seals and bearings, variable stator vanes, etc.

## REFERENCES

1. J. K. Lancaster, "CRC Handbook of Lubricants," Vol II, p. 269.
2. H. E. Sliney, Symposium on Lubricants for Extreme Environments at the ASME/ASLE Lubrication Conference, Washington, DC, October 5-7, 1982, p. 1.
3. H. E. Sliney, NASA TM D-5301, 1969.
4. J. P. King and N. H. Forster, "Synthesis and Evaluation of Novel High Temperature Solid Lubricants," AIAA Paper 90-2044 (1990).

5. J. S. Zabinski, M. S. Donley, V. J. Dyhouse, and N. T. McDevitt, "Chemical and Tribological Characterization of PbO-MoS<sub>2</sub> Films Grown by Pulsed Laser Deposition", *Thin Solid Films*, 214 (1992) 156-163.
6. M. B. Peterson, S. Z. Li, and S. F. Murray, "Wear Resistant Oxide Films for 900°C", Final Report, Argonne National Laboratory, Subcontract No. 20082401, ANL/OTM/CR-5 (1994).
7. R. F. Bunshah et al., "Deposition Technologies for Films and Coatings: Developments and Applications," Noyes Publications (1982).